NOAA Technical Memorandum NMFS F/NWC-57

Numerical Simulation of the Effect of Interannual Temperature Fluctuations on Fish Distribution in the Eastern Bering Sea

by
Nancy Pola Swan
and
W. James Ingraham, Jr.

May 1984

U.S. DEPARTMENT OF COMMERCE
National Oceanic and Atmospheric Administration
National Marine Fisheries Service

This document is available to the public through:

National Technical Information Service
U.S. Department of Commerce
5285 Port Royal Road
Springfield, VA 22161

NUMERICAL SIMULATION OF THE EFFECT OF INTERANNUAL TEMPERATURE FLUCTUATIONS ON FISH DISTRIBUTION IN THE EASTERN BERING SEA

by

Nancy Pola Swan
and
W. James Ingraham, Jr.

Resource Ecology and Fisheries Management
Northwest and Alaska Fisheries Center
National Marine Fisheries Service
National Oceanic and Atmospheric Administration
2725 Montlake Boulevard East
Seattle, WA 98112

May 1984

CONTENTS

ABSTRACT

The effects of extreme interannual temperature fluctuations (i.e., a very cold or warm year) on the Bering Sea ecosystem were examined using the Dynamical Numerical Marine Ecosystem Simulation (DYNUMES) model, originally developed at the Northwest and Alaska Fisheries Center (NWAFC) by Dr. Taivo Laevastu. The model was run using long-term monthly mean temperature fields to establish mean monthly temperature-induced migration patterns. Changes in these patterns caused by extreme temperatures were simulated by replacing the mean input temperature fields with temperature fields representative of, first, an extremely cold year, and, second, an extremely warm year.

Temperature observations for 1932 through 1982 were accessed to create monthly temperature anomaly fields over the DYNUMES model eastern Bering Sea 24x24 grid. The data reflect some persistent warm or cold conditions lasting from 2 to 5 years, evident since the late 1960s. The year 1976 was chosen as a representative cold year and 1981 as a representative warm year because they had the greatest number of data observations of all extreme years.

In the DYNUMES ecosystem simulation, fish migrate away from areas of unfavorable temperature (i.e., if the temperature falls below or rises above the "temperature tolerance" limits of a given species). Simulated temperature-induced migrations of pelagic species during late summer and autumn were similar during the cold and warm years. Simulated migrations of demersal species groups (those reacting to bottom temperatures) during the warm year were restricted to a small midshelf region where a cold core of water (<2°C) remains throughout the year. Simulated spring migrations into Bristol Bay, Alaska, began during April for the mean and warm year runs. However, in the cold year simulated migrations into Bristol Bay were delayed until June.

Field survey data for walleye pollock, _Theragra chalcogramma_, and for yellowfin sole, _Limanda aspera_, taken during May and June of 1981 and 1976 were compared with model results.

Station data in the region inshore of long. 166°42'W and north of lat. 56°43'N (Bristol Bay) during the 2 years were tabulated. During May of the cold year (1976), catches of yellowfin sole were minimal, and only a trace of pollock was found in the region. By June, however, the yellowfin catches had increased (with an average station biomass of 81.8 kg/ha), but pollock catches were still minimal. During the warm year (1981), pollock and yellowfin sole were caught at all stations sampled during May. In June, yellowfin sole catches increased, and pollock catches decreased. These data support simulated results (early migration into Bristol Bay in a warm year, later during a cold year).

INTRODUCTION

The broad, resource rich continental shelf of the eastern Bering Sea provides a choice location for studies of ecosystem complexities. Computer simulation modeling is one of the strongest tools we can use to increase our understanding of the multicomponent interactions inherent in such an ecosystem. The present study uses the DYNUMES (Dynamical Numerical Marine Ecosystem Simulation) model, developed at the Northwest and Alaska Fisheries Center (NWAFC) by Dr. Taivo Laevastu, along with 50 years of eastern Bering Sea temperature observations to examine relationships between interannual temperature fluctuations and migration patterns of selected species groups in the eastern Bering Sea.

The purpose of simulation modeling is to determine the dynamics and to prioritize the forcing functions controlling a system's behavior. Initial assumptions of dynamics are based on existing knowledge, field (empirical) data, and theoretical studies. Initial values of model inputs such as biomass and temperature, and of parameters such as growth rate, are estimated from the best available data. The model is allowed to run its course and generate data fields of the component(s) of interest for as long as desired. Results can then be compared to independently measured conditions in nature to test assumptions.

Migrations induced by temperature changes have recently been simulated with DYNUMES (Swan 1983). Anomalously warm or cold years can affect the timing and/or magnitude of biological events. In the present study, effects of extreme annual temperatures on the ecosystem have been simulated with DYNUMES by replacing the long-term monthly mean input temperature fields with temperature fields representative of, first, an extremely cold year, and, second, an extremely warm year.

We will first discuss the calculation of input temperature fields (surface and near bottom temperatures representative of the mean, a typical cold year, and a typical warm year) used in the analysis. A brief overview of the DYNUMES simulation model is presented next, with emphasis on the modeled effects of temperature and the simulation of fish migrations. Finally, results of the model simulations are presented and are discussed in conjunction with field observations from research surveys.

EASTERN BERING SEA TEMPERATURE FIELDS

Data Base

The historical eastern Bering Sea temperature record began with only 15 stations in 1932; however, station coverage was greatly increased during periods beginning in 1953, 1966, and 1974 (Table 1). A data base containing available randomly spaced surface and near-bottom temperature observations resides on the NWAFC Burroughs 7800 computer.1/ All data through 1979 (approximately 19,000 observations) were seasonally averaged over 1° x 1/2° squares (Ingraham 1981a) and used to describe the mean seasonal eastern Bering Sea surface and near-bottom temperature patterns (Ingraham 1981b).

The data base has recently been updated through 1982 and now contains approximately 25,000 observations. Ingraham (1983) mapped these updated observations onto the equal area eastern Bering Sea grid used in the DYNUMES simulation model (Fig. 1; see section 3 for a description of the model). He calculated the long-term monthly mean surface and bottom temperatures as well as monthly anomalies by year over the DYNUMES grid. Since the results of the Ingraham (1983) analysis are used in the present study, a brief description of his methods follows.

The latitude and longitude of each data observation is used to determine the four closest adjacent grid points. A weighting factor inversely proportional to the square of the distance from the observation point is computed at each of the four grid points, where the weights for the four grid points total 1.0. After all data from one month have been processed, the sum of the

---

1/ Reference to trade name does not imply endorsement by the National Marine Fisheries Service, NOAA.

2:43.7.17e

Table 1.--Number of historical eastern Bering Sea surface temperature observations by year and month.

Year	Month												
	1	2	3	4	5	6	7	8	9	10	11	12	Total
1932	0	0	0	0	0	0	3	43	10	0	0	0	56
1933	0	0	0	0	0	0	17	30	0	0	0	0	47
1934	0	0	0	0	0	0	36	66	0	0	0	0	102
1935	0	0	0	0	0	0	9	23	0	0	0	0	32
1936	0	0	0	0	0	0	1	3	0	0	0	0	4
1937	0	0	0	0	0	80	52	10	18	0	0	0	160
1938	0	0	0	0	0	0	0	119	72	0	0	0	191
1939	0	0	0	0	14	91	139	110	6	0	0	0	360
1940	0	0	0	0	0	0	71	113	0	0	0	0	184
1941	0	0	0	0	27	11	39	0	0	0	0	0	77
1942	0	0	0	0	0	0	0	0	0	0	0	0	0
1943	0	0	0	0	0	0	0	0	0	0	0	0	0
1944	0	0	0	0	0	0	0	0	0	0	0	0	0
1945	0	0	0	0	0	0	0	0	0	0	0	0	0
1946	0	0	0	0	0	0	0	0	0	0	0	0	0
1947	0	0	0	0	0	0	8	4	1	0	0	0	13
1948	0	0	0	0	0	0	7	13	0	0	0	0	20
1949	0	0	0	0	0	0	25	42	0	0	0	0	67
1950	0	0	0	0	0	0	0	0	0	0	0	0	0
1951	4	22	0	0	0	0	0	0	0	0	0	0	26
1952	0	0	0	0	0	0	0	0	0	0	0	0	0
1953	0	0	0	0	1	0	15	125	35	0	0	0	176
1954	0	0	0	3	35	13	42	17	44	0	0	0	154
1955	0	0	24	40	20	43	11	17	11	0	0	0	166
1956	0	0	0	0	0	12	62	62	24	0	0	0	160
1057	0	0	0	0	0	43	66	92	0	0	0	0	201
1958	0	0	0	1	3	56	108	32	6	0	3	0	209
1959	0	0	1	0	0	116	116	46	20	2	0	0	301
1960	3	18	0	0	0	39	173	51	19	16	0	0	319
1961	0	0	40	68	26	121	113	83	147	7	0	0	605
1962	0	0	4	0	24	42	77	10	195	0	0	0	352
1963	0	0	2	0	12	64	86	13	14	0	4	0	195
1964	0	0	41	33	37	53	75	18	9	1	2	0	269
1965	0	0	5	12	1	98	121	41	1	0	0	0	279
1966	9	7	0	2	70	256	171	69	2	1	0	0	587
1967	0	0	11	0	8	204	215	55	7	0	0	0	500
1968	0	42	0	1	0	160	253	26	15	2	0	0	499
1969	13	15	8	111	70	204	203	89	2	0	0	0	715
1970	9	24	28	38	50	188	142	100	103	12	0	0	694
1971	1	6	9	27	46	396	81	89	58	2	0	0	695
1972	0	13	10	26	53	166	133	77	44	19	0	3	544
1973	0	5	4	50	63	165	209	43	29	24	4	0	596
1974	0	3	18	51	42	163	263	80	3	22	12	0	657
1975	15	13	21	15	96	283	221	350	362	148	77	0	1601
1976	10	7	74	164	342	472	211	218	321	184	0	0	2003
1977	0	1	16	61	220	136	224	186	124	33	0	0	1001
1978	0	89	20	202	294	466	415	70	90	0	0	0	1646
1979	0	14	41	115	196	381	512	315	0	0	0	0	1574
1980	21	14	0	0	137	193	103	126	71	0	0	0	665
1981	17	195	48	0	247	198	223	43	56	95	52	0	1174
1982	0	0	0	13	91	198	308	197	142	322	0	0	1271
Total	102	488	425	1033	2225	5111	5359	3296	2061	890	154	3	21147

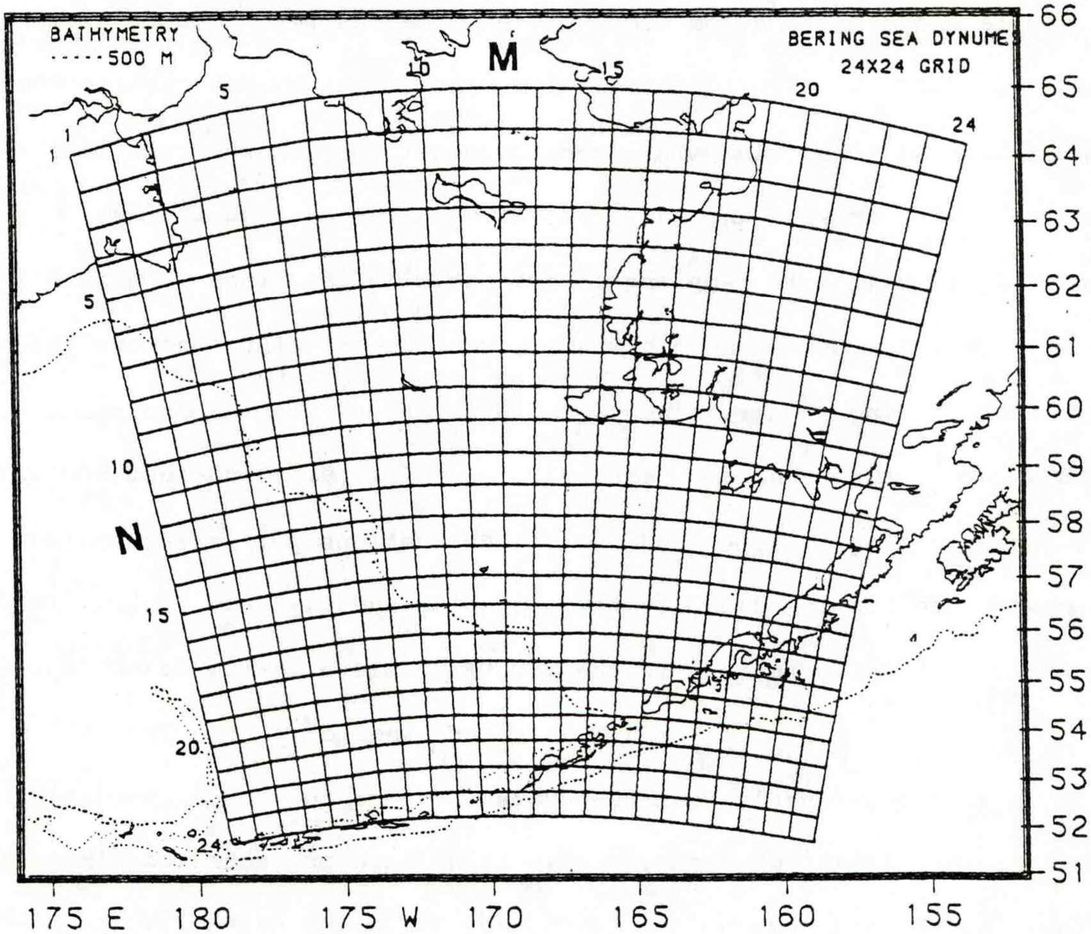

Figure 1.--Mercator projection of DYNUMES eastern Bering Sea 24x24 grid.

weighted data values at each grid point is divided by the sum of the weights at that grid point to give the mean surface or bottom temperature at the grid point. Data gaps were filled with spatial and temporal (i.e., month-to-month) interpolations. The resulting "smoothed" monthly mean temperature fields were checked for consistency with known local meteorlogical patterns.

Surface and near-bottom temperature anomalies were computed for each month and year at all grid points with data values by subtracting the mean temperature at that grid point from the observed temperature. Data are sparse in any one year and month as shown in Table 1; on the average, a seasonal inequality in sampling is evident with less than 10 stations per month taken from late autumn through winter, while nearly 100 stations per month were taken during summer. The number of stations sampled increased over time, with about 100 stations per year by 1953, an increase to about 500 stations per year starting in 1966, and over 1,000 stations per year from 1974 to 1982. To compensate for low data density, Ingraham averaged the monthly temperature anomalies over nine regions in the DYNUMES eastern Bering Sea grid (Fig. 2).

Mean Temperature Regime

The analyzed monthly mean temperature fields for March (winter) and August (summer) adapted from Ingraham (1983) are presented for the sea surface (Figs. 3a, 3b) and near-bottom (Figs. 4a, 4b). The extent of ice cover over the shelf area in the northeastern Bering Sea during winter can be delineated by the position of the -1°C isotherm in the surface field (Fig. 3a). The effect of the ice cover on the bottom waters is reflected in the very low (<0°C) temperatures in shallow areas (Fig. 4a). Mean surface temperature during summer (Fig. 3b) reaches a maximum of 10-12°C near shore along the west coast of Alaska and offshore in the central basin. The two warm regions

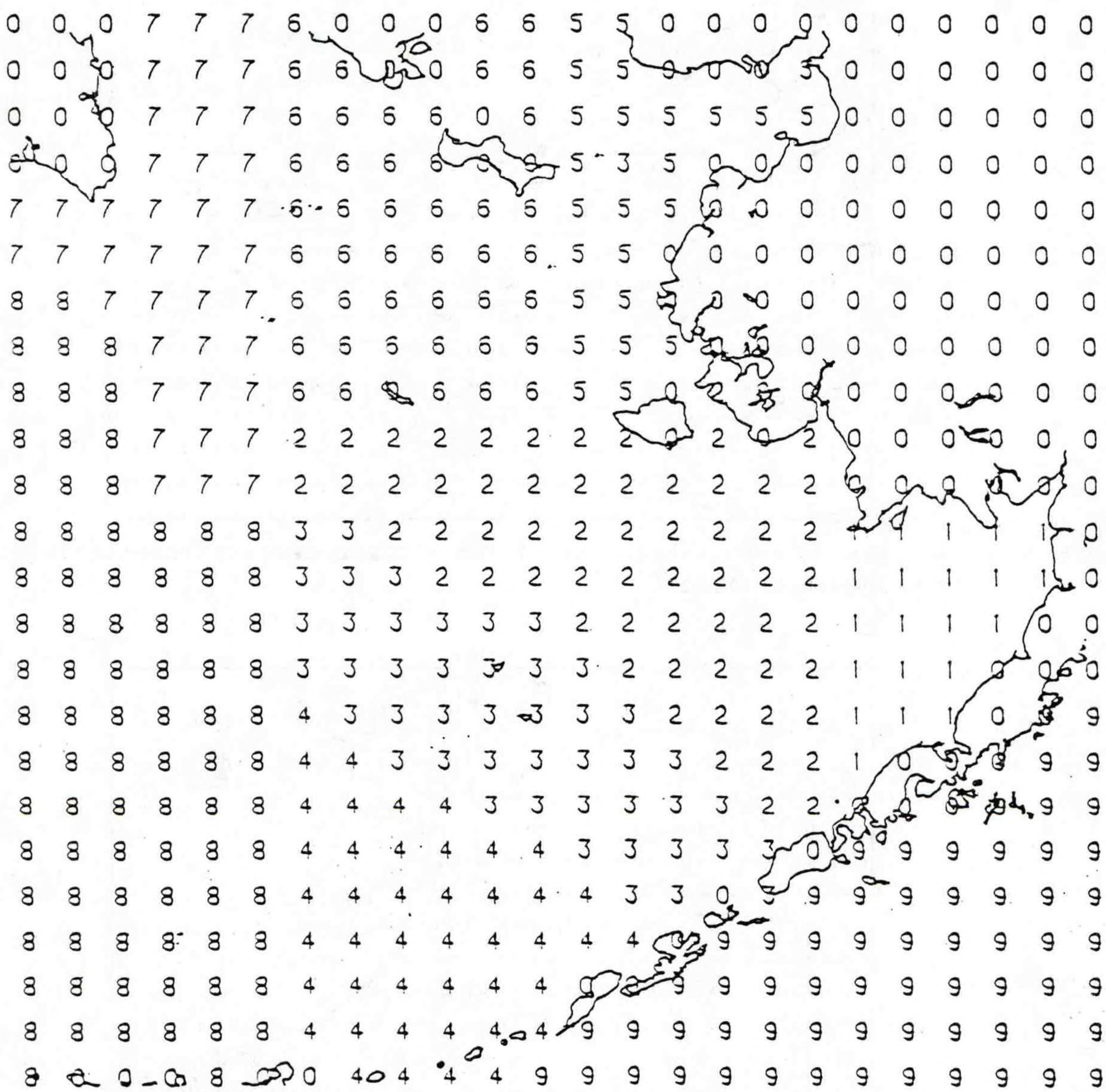

Figure 2.--DYNUMES Bering Sea land-sea regions.

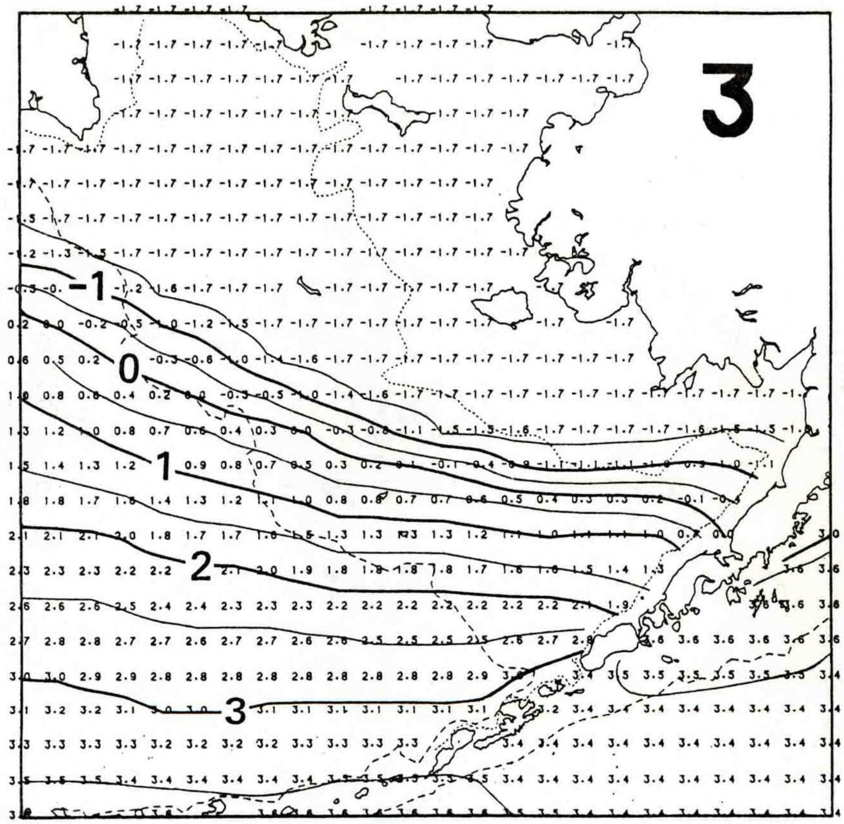

Figure 3a.--Mean Bering Sea winter (March) sea surface temperatures (adapted from Ingraham 1983).

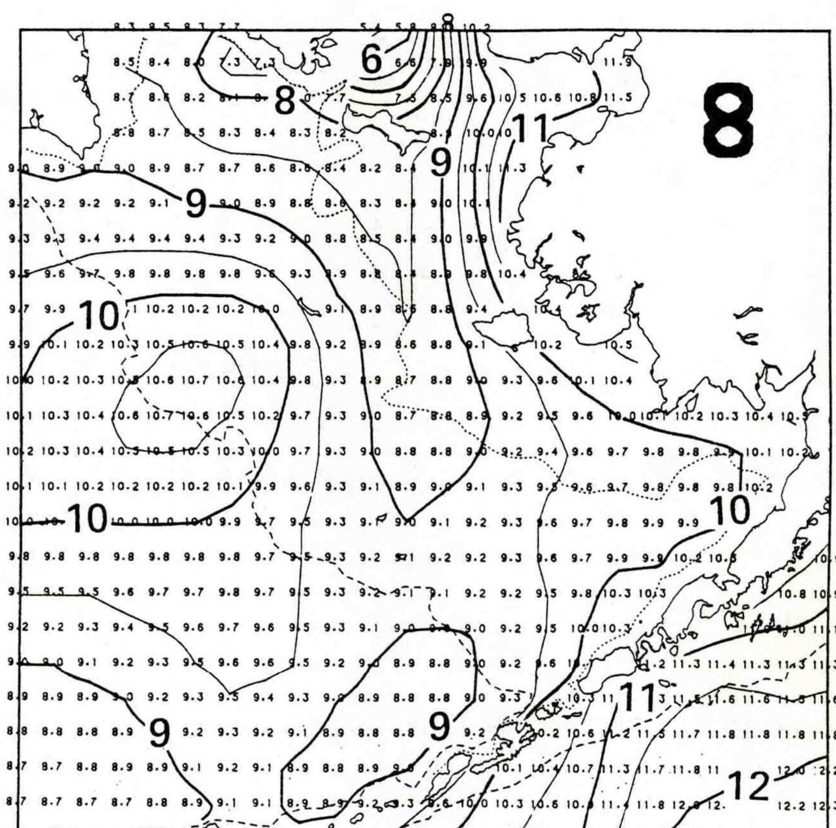

Figure 3b.--Mean Bering Sea summer (August) sea surface temperatures (adapted from Ingraham 1983).

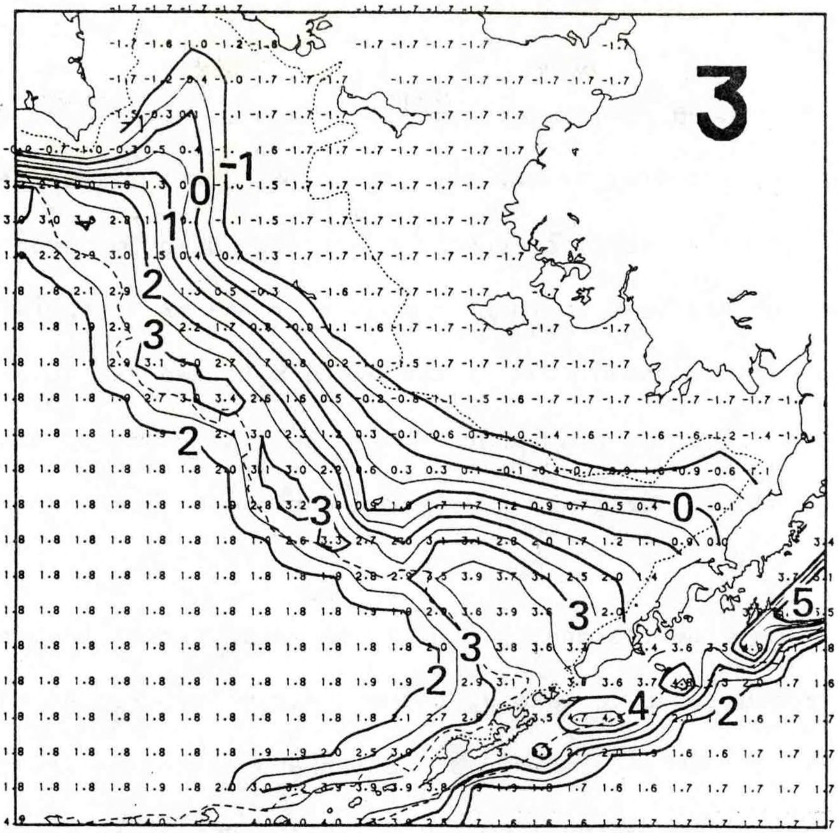

Figure 4a.--Mean Bering Sea winter (March) bottom temperatures (adapted from Ingraham 1983).

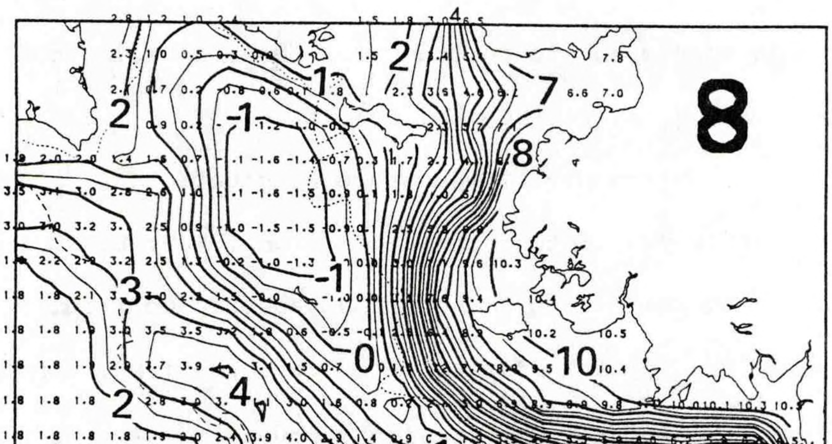

Figure 4b.--Mean Bering Sea summer (August) bottom temperatures (adapted from Ingraham 1983).

are separated by a band of lower temperature (8-9°C) water over the midshelf. The mean summer near-bottom temperature field (Fig. 4b) illustrates that a mid-shelf core of cold (<2°C) near-bottom water, remnant of winter cooling, remains throughout the year south of the Gulf of Anadyr. Otherwise, the mean near-bottom temperature over most of the eastern Bering Sea during summer is between 2° and 4°C, except near shore along the west coast of Alaska, where water of up to 10°C is uniformly mixed from surface to bottom by strong tidal currents.

The transition from the mean winter to the mean summer temperature regime occurs rapidly during late spring and early summer. At the surface, the warming trend is in a northward direction and isotherms are zonally flat until June. The warming of near-bottom waters occurs first along the coast and then progresses offshore. The summer regime gradually cools during autumn, with ice cover returning (on the average) in November. These transition periods correspond to periods of increased biological activity, including fish spawning, migrating, and foraging.

Interannual Temperature Fluctuations

The time series of temperature anomalies from 1950 through 1982 averaged over three regions in the Bering Sea for the sea surface (Fig. 5) and for near-bottom water (Fig. 6) are adapted from Ingraham (1983). Region 1 roughly corresponds to Bristol Bay, region 2 covers the southern midshelf, and region 3 includes the southern outer shelf and slope (Fig. 2).

The general structure of the temperature anomaly time series shown in Figures 5 and 6 is similar in the surface and bottom layers in regions 1 and 2. The bottom water in region 3, however, is below the pycnocline and is less affected by sea surface temperature changes. The range in data values

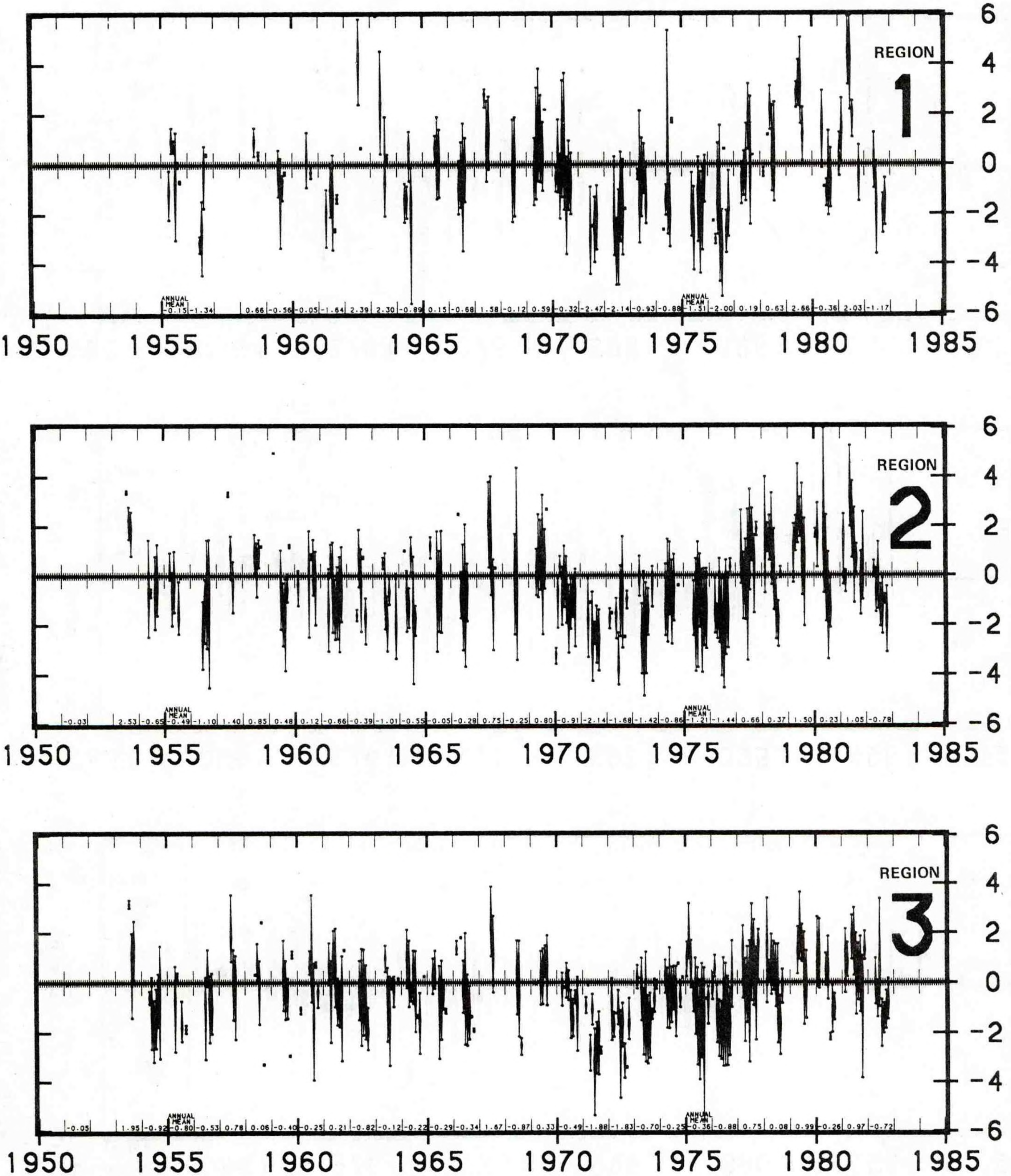

Figure 5.--Time series from 1950 to 1982 of ranges and average sea surface temperature anomalies for region 1, 2, and 3 of the DYNUMES grid.

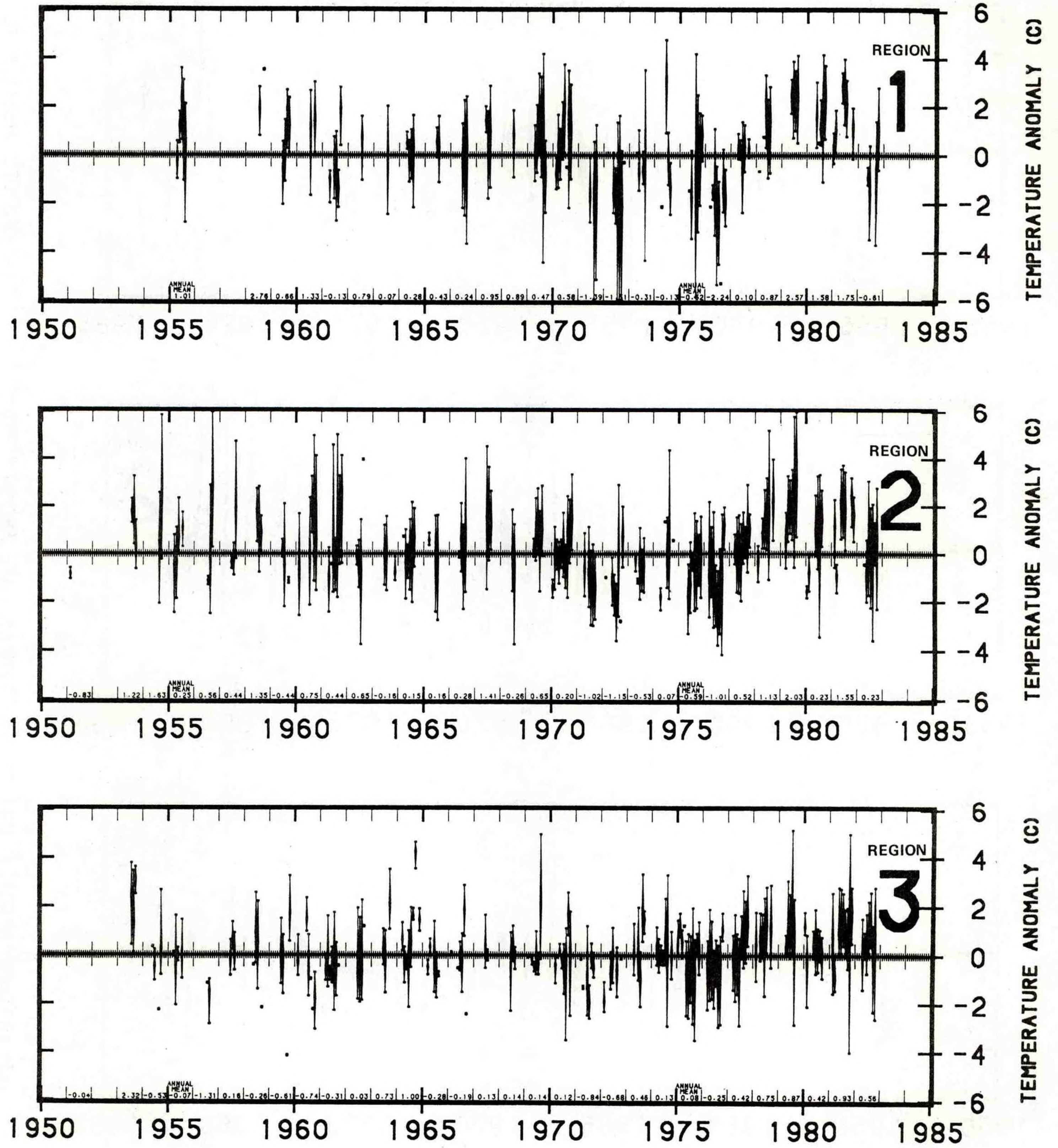

Figure 6.--Time series from 1950 to 1982 of ranges and average near bottom temperature anomalies for region 1, 2, and 3 of the DYNUMES grid.

is greatest in both the surface and bottom waters in region 1, due to the larger range of air temperatures near the continental boundary and to the strong vertical mixing within Bristol Bay.

Figure 5 illustrates a pronounced interannual surface warming and cooling cyclic pattern beginning in the late 1960s. Prior to that time, no pronounced pattern is evident, demonstrating that either the local atmospheric circulation (and, therefore, sea surface temperature) patterns have changed in recent decades (which is very unlikely), or that sparsity of data prior to 1966 (especially during winter months) inhibits the detection of dominant cyclic patterns. The interannual cyclic pattern is less pronounced in the bottom waters (Fig. 6) and is barely evident at the outer shelf (region 3).

The cyclic pattern evident in the regionally averaged surface temperatures (Fig. 5) begins with a warming trend in 1967. The trend is evident at the inshore stations (regions 1 and 2) for several months; farthest inshore in Bristol Bay (region 1), extreme temperatures persist through 1970. The trend reverses in the early 1970s; the coldest years are 1971, 1972, and 1976. Warming resumes in 1977 with maximum temperatures occurring in 1979 and 1981.

Temperature Anomaly Fields for Model Input

The DYNUMES simulation model uses gridded surface and bottom temperature fields for each monthly time step in the calculations of several biological processes, as described in section 3. In order to investigate the effects of anomalous temperatures on ecosystem simulations, 2 years of monthly temperature fields were prepared for 1976 and 1981, representing an extremely cold year and an extremely warm year, respectively. Although equally extreme temperatures occurred in other years, 1976 and 1981 had greater numbers of data observations

(Table 1). Data gaps were filled by the same procedure used to smooth the mean temperature fields; however, regional means were assigned as initial values. Resultant fields were verified using general wind circulation patterns determined from daily sea surface pressure maps (Ingraham et al., 1983). Examples of actual temperature anomaly distributions and the smoothed anomaly fields for the same months are shown in Figures 7a and b (winter, 1976), Figures 8a and b (summer, 1976), Figures 9a and b (winter, 1981), and Figures 10a and b (summer, 1981).

The smoothed monthly temperature anomaly fields for 1976 and for 1981 were added to the smoothed monthly mean temperature fields (from Ingraham 1983) to form annual series of extreme surface and near-bottom temperature fields to be input to the DYNUMES simulation model. These monthly surface and near-bottom temperature fields (smoothed anomaly fields plus smoothed mean fields) for 1976 (cold year) and 1981 (warm year) are presented in the appendices.

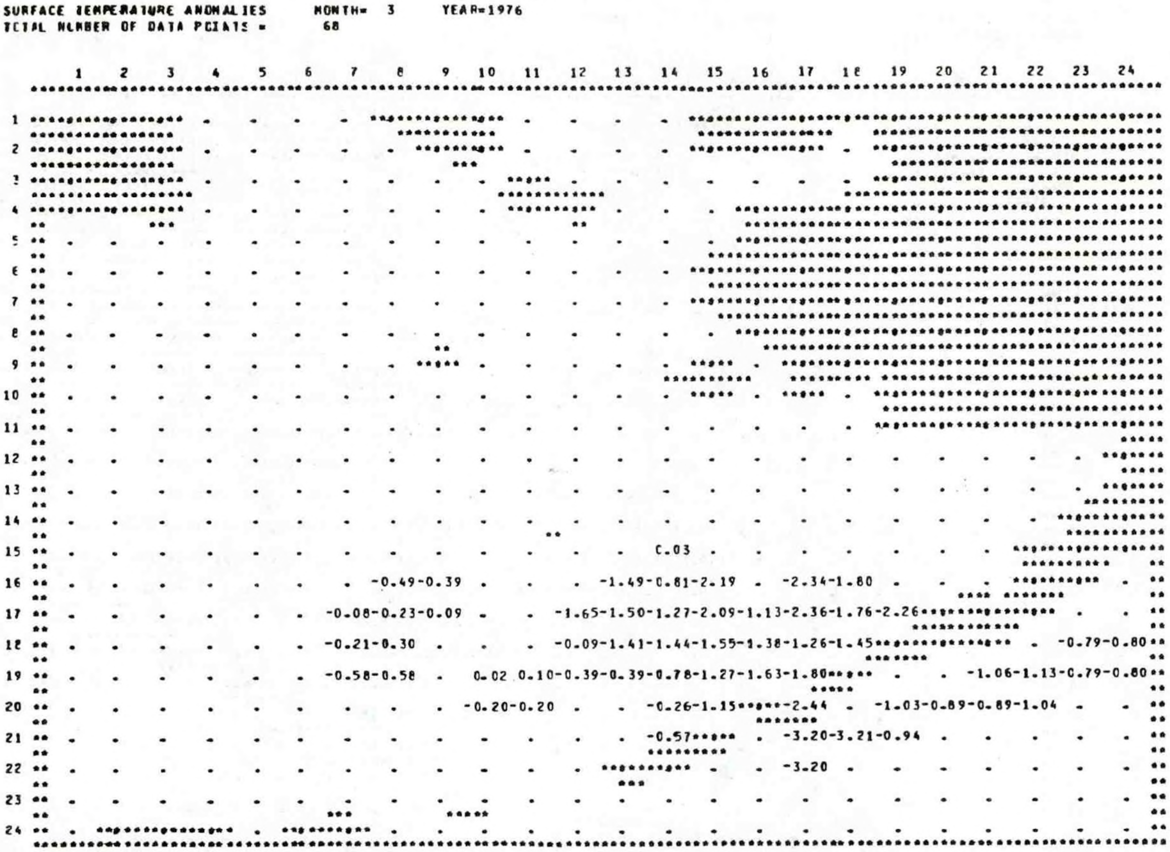

Figure 7a.--Anomalies of observations of sea surface temperature for March 1976.

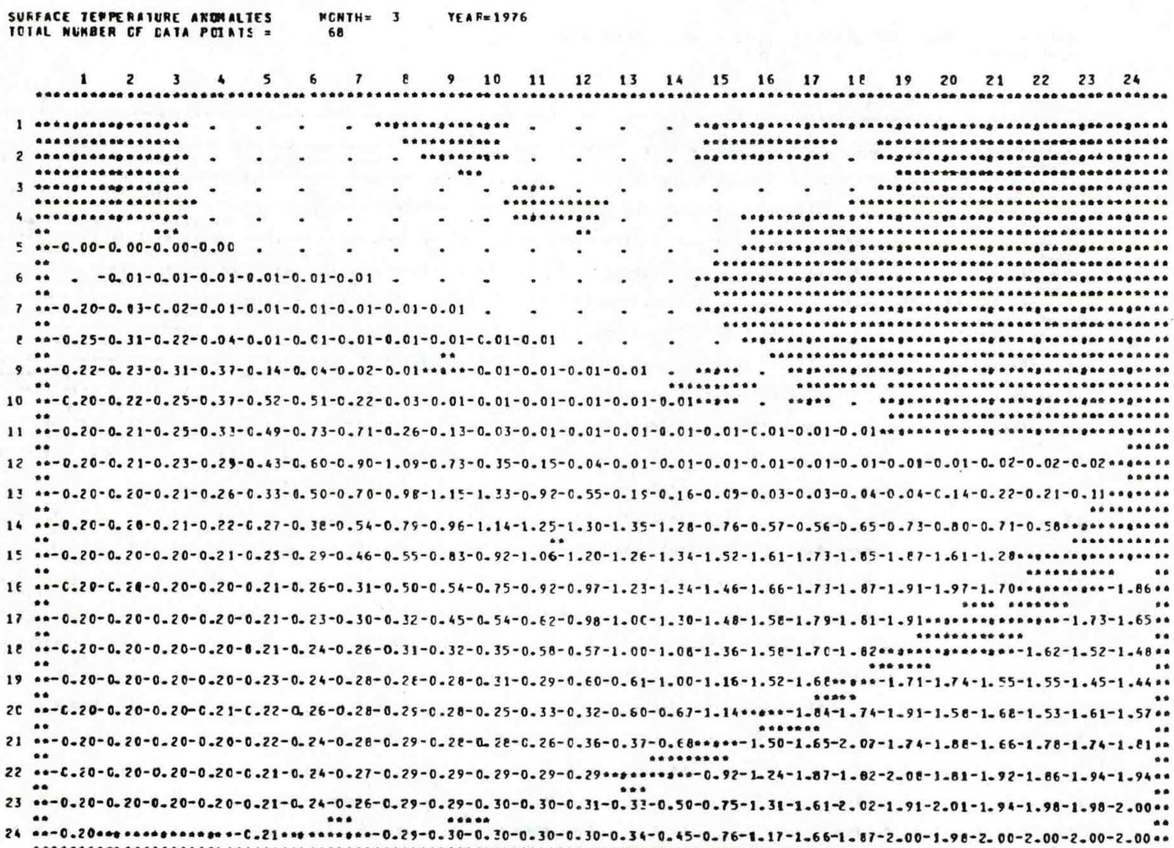

Figure 7b.--Smoothed sea surface temperature anomaly field for March 1976.

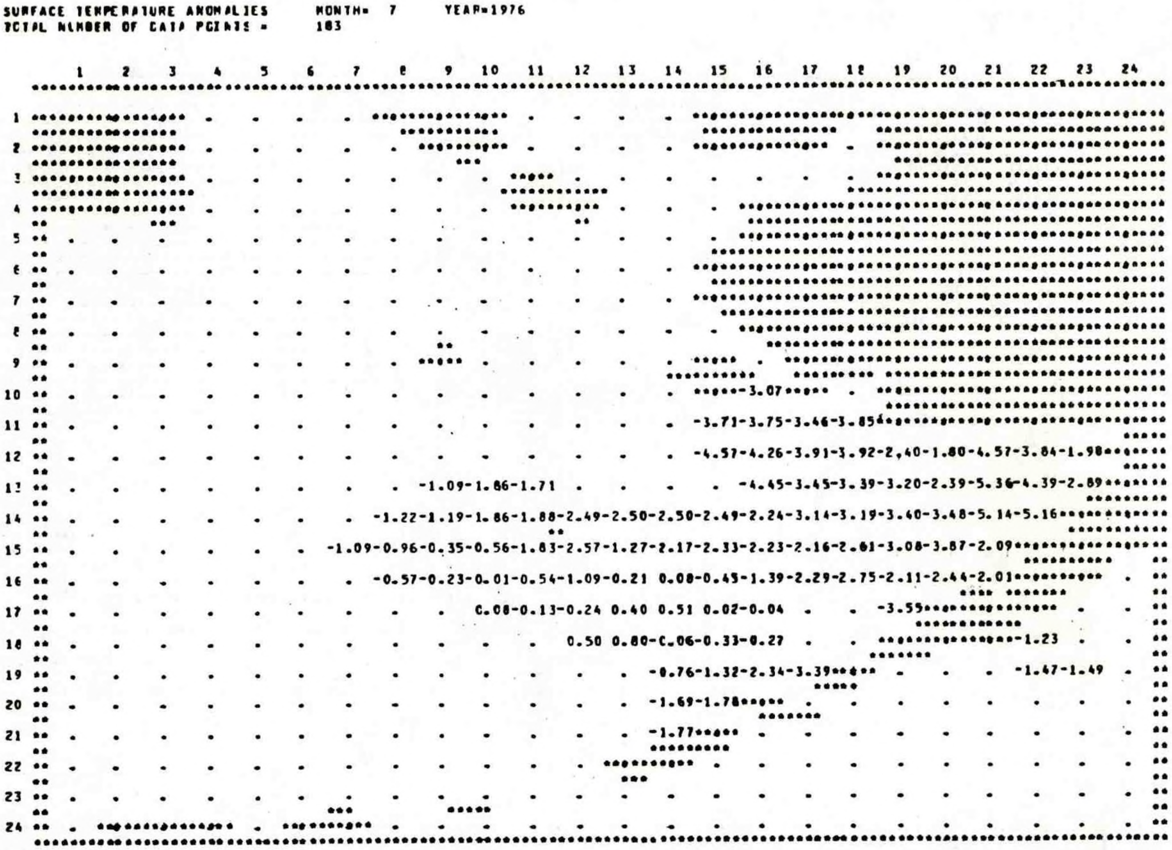

Figure 8a.--Anomalies of observations of sea surface temperatures for July 1976.

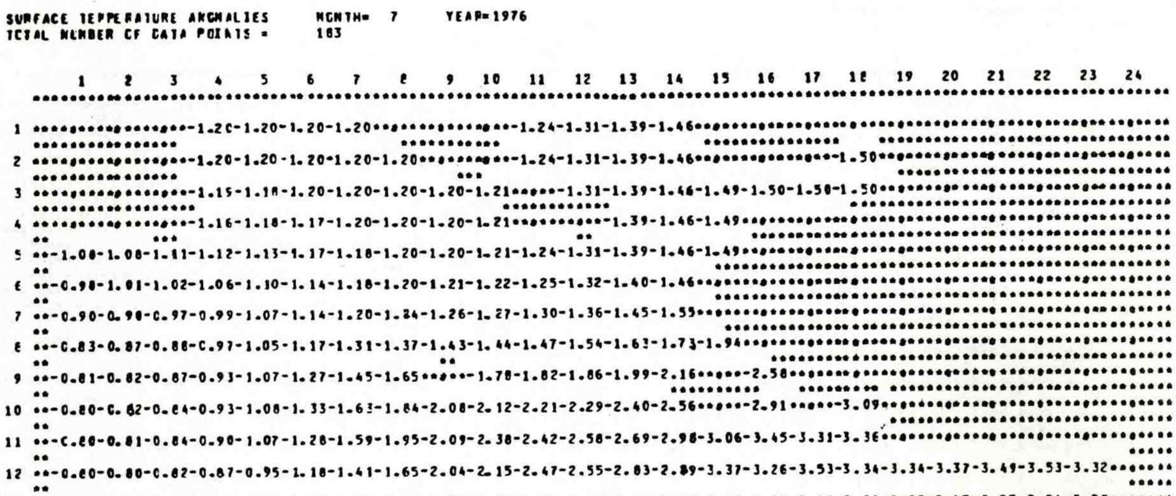

Figure 8b.--Smoothed sea surface temperature anomaly field for July 1976.

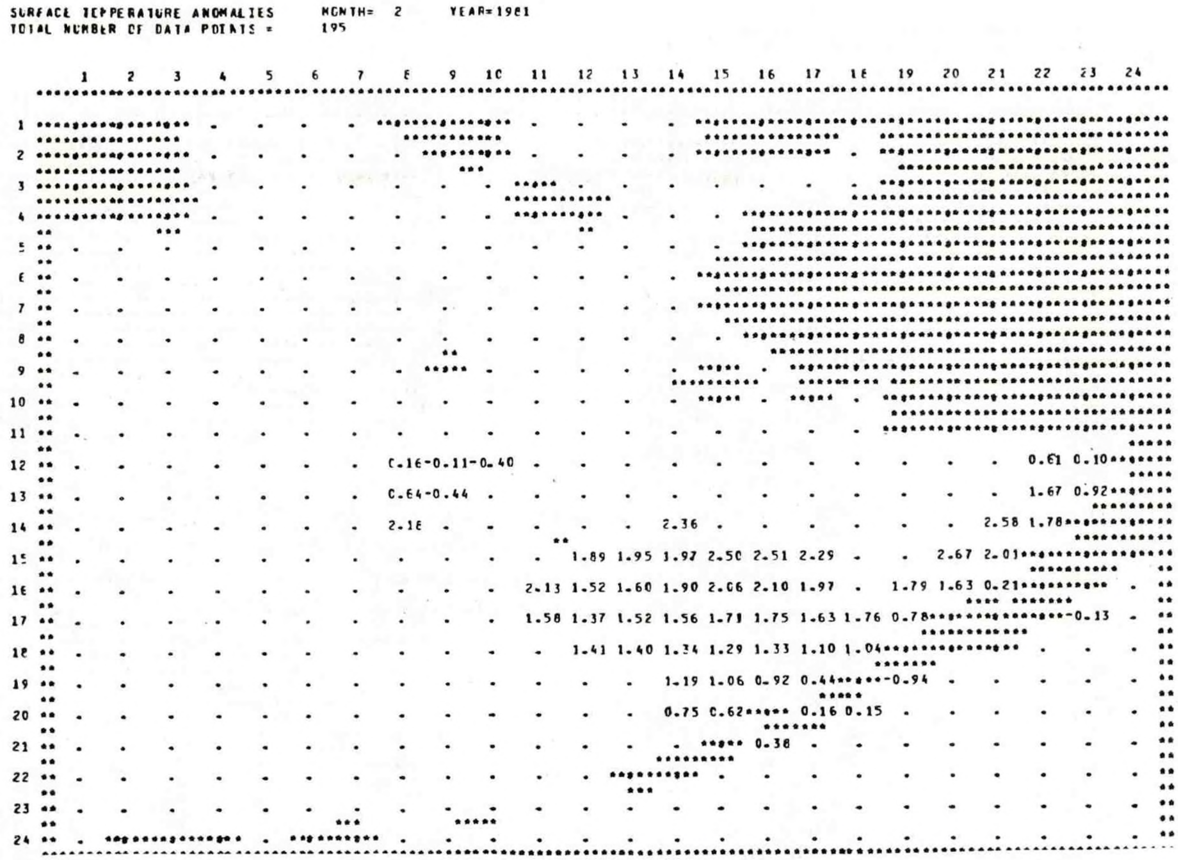

Figure 9a.--Anomalies of observations of sea surface temperature for February 1981.

Figure 9b.--Smoothed sea surface temperature anomaly field for February 1981.

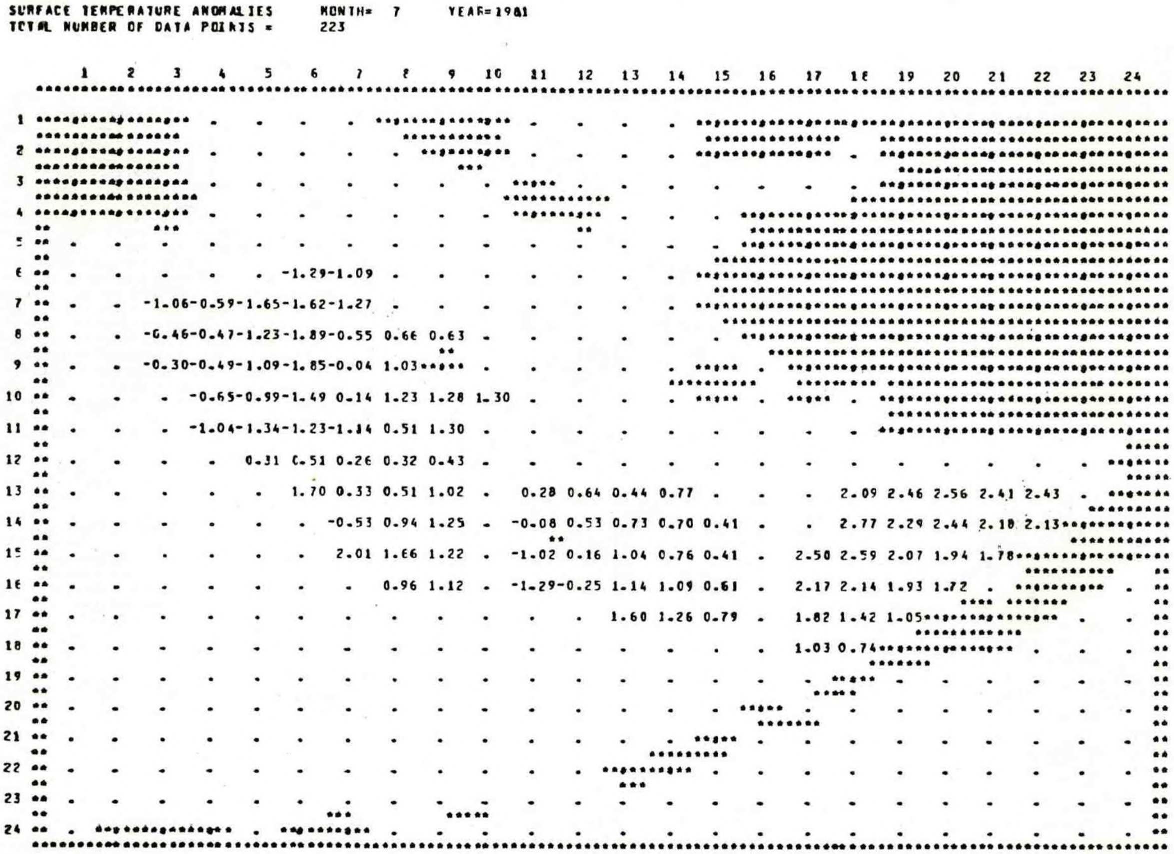

Figure 10a.--Anomalies of observations of sea surface temperatures for July 1981.

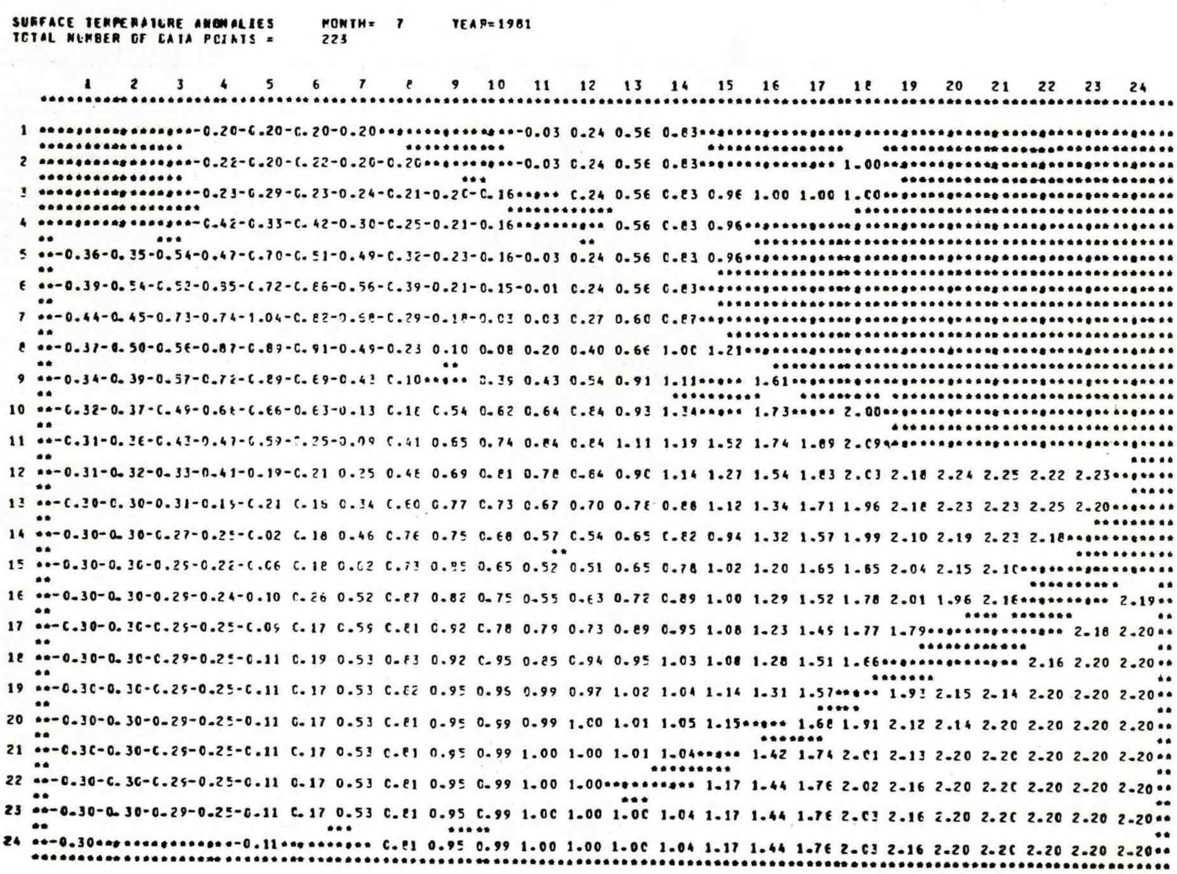

Figure 10b.--Smoothed sea surface temperature anomaly field for July 1981.

ECOSYSTEM SIMULATION

Sequence of Model Calculations

The DYNUMES simulation model was created by Dr. Taivo Laevastu at NWAFC, and has been used extensively to study ecosystem interactions in the eastern Bering Sea (e.g., Laevastu and Favorite 1978, 1979; Laevastu et al. 1976; Laevastu and Marasco 1982). The model calculations are performed each month over the eastern Bering Sea 24x24 grid with an area of over one million square kilometers (Fig. 1). Simulated model processes for each species (Table 2) include growth, apex predation by birds and mammals, inter- and intra-species predation and competition for food, and fishing mortality. In addition, the model simulates the temporal and spatial variability resulting from fish migrations. During each model time step, these processes are computed at each grid point.

The general model flow is depicted in Figure 11. The main program reads input parameters and data fields, including monthly surface and bottom temperature arrays, and then directs program flow by calling other subroutines. The consumption of each fish species by birds and mammals is computed in BIRMAM, the first subroutine called. Next, phyto- and zooplankton biomasses are computed in subroutine PLANKT. Fish migrations are simulated in subroutine MIGR. Seasonal migrations with predictable spatial and temporal patterns (e.g., spawning migration) are computed separately from temperature-induced migrations. The final subroutine called by the main program is FEDGRO, which computes fish predation and calls PUGIMO, which calculates growth and adjusts the biomass for fishing mortality. Comprehensive discussions of the model can be found in Laevastu and Larkins (1981) and in Gallagher (1983).

Table 2.--Species groups in the DYNUMES simulation model.

Species group no.	Species
1-4	Used for special study
5	Pacific halibut
6	Flathead sole, flounder
7	Yellowfin, rock sole
8	Other flatfish
9	Pacific ocean perch
10	Sablefish
11	Cottids and other demersal species
12	Walleye pollock
13	Pacific cod, saffron cod
14	Pacific herring
15	Capelin and other pelagic species
16	Atka mackerel
17	Salmon
18	Squids
19	King crab
20	Snow (Tanner) crab
21	Shrimp
22	Predatory benthos
23	Infauna
24	Epifauna
25	Copepods
26	Euphausiids
27	Phytoplankton

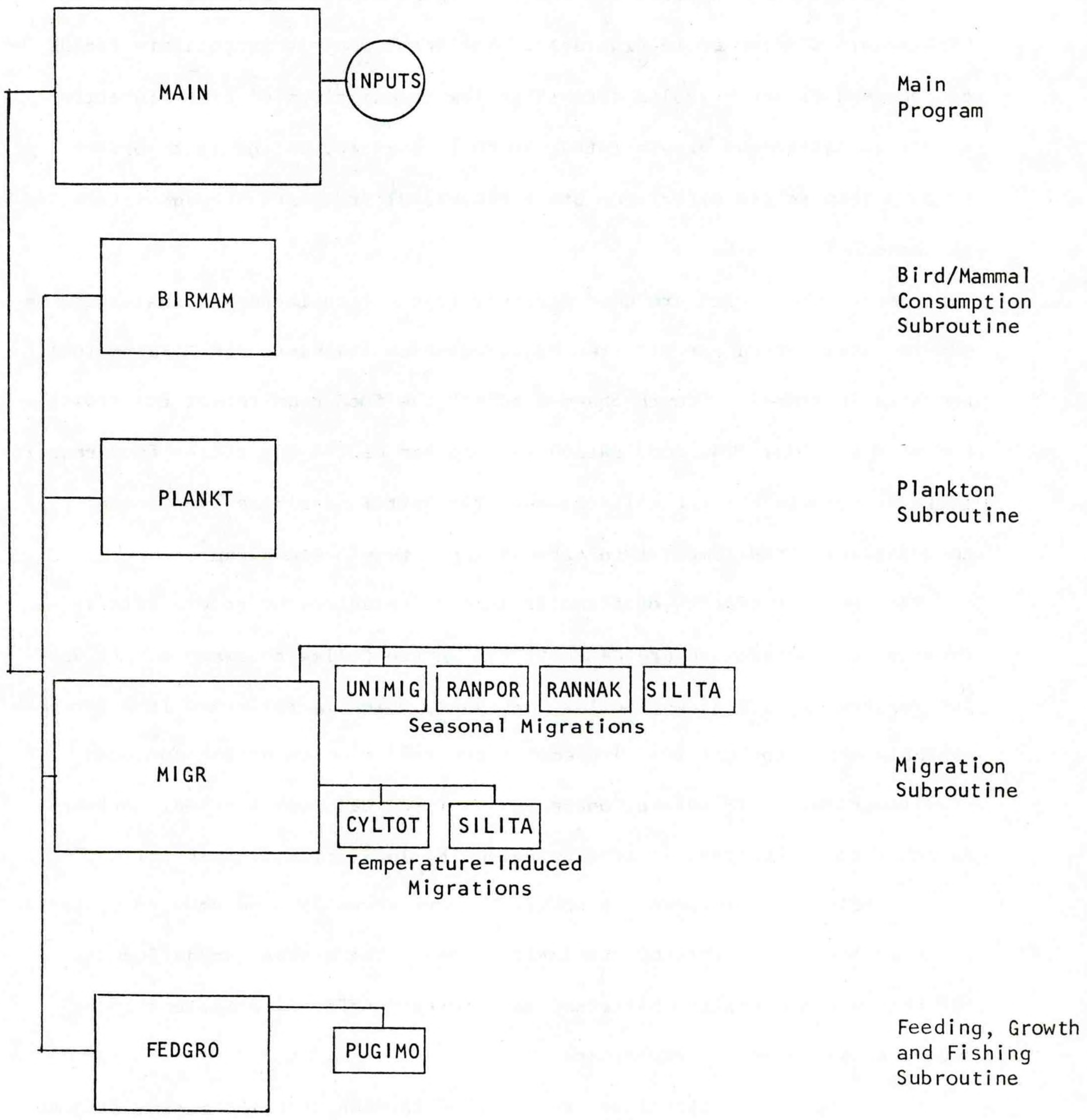

Figure 11.--Simplified flow diagram for DYNUMES simulation model.

Simulation of Temperature Effects

The direct and indirect effects of temperature on simulated processes of DYNUMES are diagrammed in Figure 12. The input monthly temperature fields can be used directly (solid arrows) in the calculations of fish migrations and/or instantaneous growth rates, which in turn induce indirect (broken arrows) temperature effects on other biological processes through interactions in the model.

Temperature fields are used directly in the formulation of instantaneous growth rates, which are affected by temperature (Laevastu and Larkins 1981; Laevastu in press). Growth changes affect the food requirement for growth for each species. The food ration is computed as the sum of the food requirements for growth and for maintenance. The latter is also a function of temperature, since temperature affects the rate of metabolism.

The indirect effects of formulating the instantaneous growth rate as a function of temperature are demonstrated in the following example. At very low temperatures, fish metabolism decreases, which is reflected in a decreased instantaneous growth rate. A predator species' biomass growth and food requirement will, therefore, decrease. A principal prey species, however, may undergo an increase in biomass caused by lower predation mortality.

The effects of temperature on growth have recently been studied by Laevastu (in press) using the PROBUB simulation model. The present study focuses on the changes in migration patterns, and indirect effects of those changes, caused by extremes in temperature.

Fish biomass distributions are modified through migrations away from areas of unfavorable temperature (i.e., outside the tolerance range for each species). The redistribution of biomass causes changes in prey availability and, therefore,

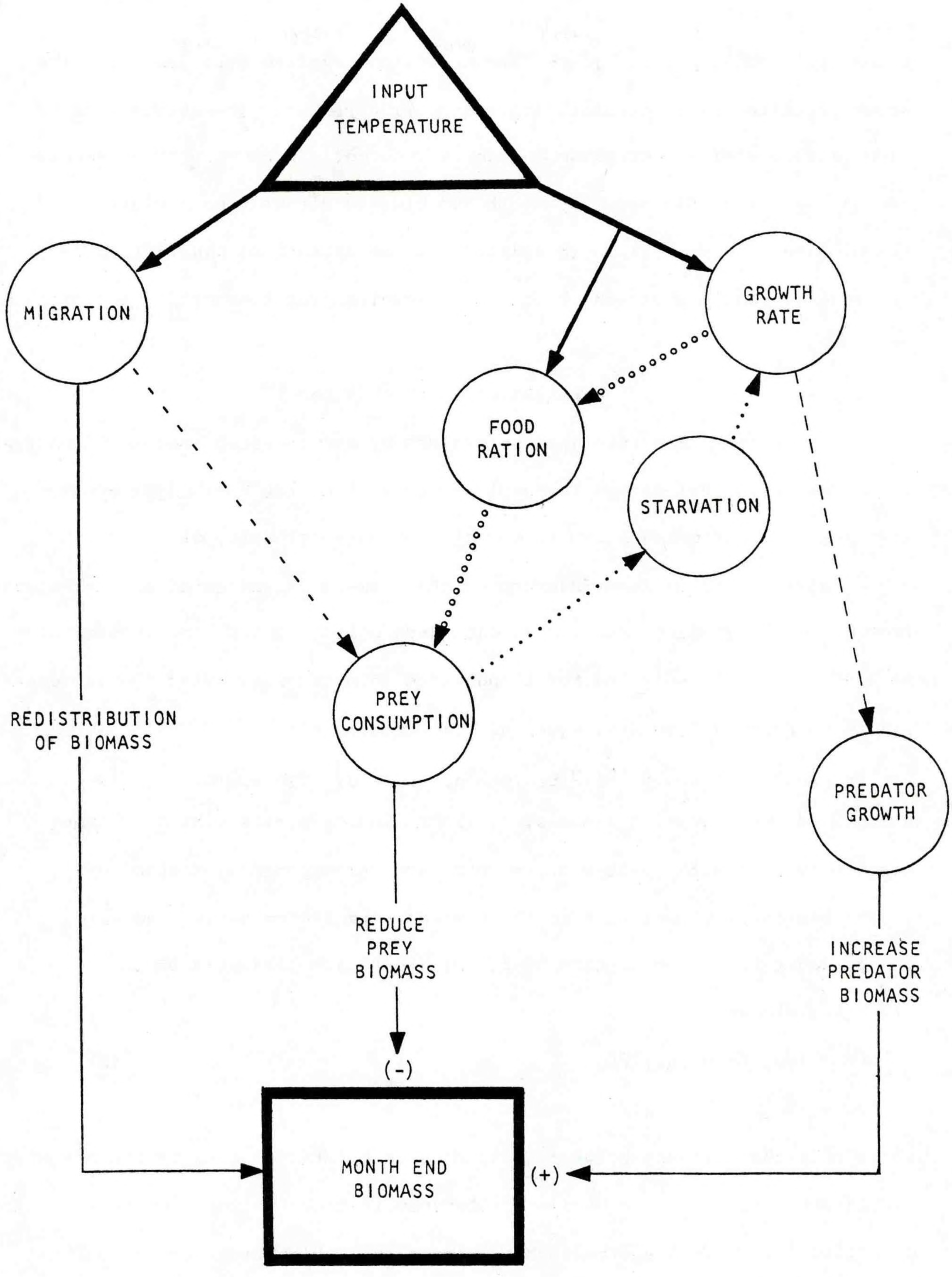

Figure 12.--Schematic of the possible effects of temperature in the DYNUMES model simulation.

alters prey consumption. If the amount of food available is less than the amount required by a predator, starvation will result. The growth rate is then recalculated and predator growth is reduced. In other words, temperature-induced fish migrations modify month-end biomass directly by redistributing the biomass over the grid. In addition, these migrations can indirectly increase or reduce month-end biomass by reducing prey consumption and predator growth.

Formulations of Migrations

Migrations are simulated in DYNUMES by a three-step process (Swan 1983). First, migration velocities (km/day) are calculated for each major species (for which migration is known to occur) at each model grid point. In the second step, the migrating fraction of the biomass is estimated and is separated from the non-migrating fraction at each grid point. Third, the biomass at each grid point is adjusted for changes due to migration, using the "upcurrent" finite difference advection equation (Laevastu 1976):

$$B_{t,n,m} = B_{t-1,n,m} - (t_d |U|_{t,n,m} BX_{n,m}) - (t_d |V|_{t,n,m,} BY_{n,m}) \qquad (1)$$

where B is the migrating biomass, t_d is the length of the migration time step, U and V are the east-west and north-south components, respectively, of the migration velocity, n is the row and m is the column of the grid point, and t is the model time step. BX and BY are gradients of the migrating biomass:

$$BX = (B_{n,m} - B_{n,m\pm1})/L \qquad (2)$$

$$BY = (B_{n,m} - B_{n\pm1,m})/L \qquad (3)$$

where L is the distance between adjacent grid points (63.5 km in the DYNUMES Bering Sea grid), and the biomass difference is taken in the "upstream" direction (i.e., in the direction of migration). Migrations are calculated using a 2-day time step ($t_d = 2$) for stability. The stability criterion is:

$$U_{max} t_d < L \qquad (4)$$

where U_{max} is the maximum magnitude of either migration velocity component. Migration calculations are performed 15 times during each monthly model time step, after which conservation of biomass is enforced, since the advection equation is not fully conservative, using the formula:

$$B_{t+\Delta t,n,m} \leftarrow R * B_{t+\Delta t,n,m} \qquad (5)$$

where

$$R = (\textstyle\sum_{n,m} B_{t,n,m})/(\textstyle\sum_{n,m} B_{t+\Delta t,n,m}). \qquad (6)$$

R is very near unity.

The resulting migration biomass is then smoothed over neighboring grid points to simulate random ("diffusive") migrations, using a five-point Laplacian diffusion equation:

$$B_{n,m} = \alpha\ B_{n,m} + 1/4(1 - \alpha)[B_{n-1.m} + B_{n,m-1} + B_{n,m+1}] \qquad (7)$$

where α is a species-specific parameter designating the degree of smoothing desired (α=1 for no smoothing and α = 0 for maximal smoothing). Typical values for α are between 0.7 and 0.9. Finally, the migrated biomass is added to the nonmigrating biomass at each grid point.

The computational procedures for the simulation of both seasonal and temperature-induced migrations are similar; that is, the same steps are followed. In the latter case, however, the initial estimate of velocity, the final velocity field, and the migrating fraction of the biomass are all functions of temperature. The model compares the input temperature at each grid point to the maximum and minimum tolerance temperatures for each species to determine if migration will occur. Either the surface or bottom temperature field is used, depending on whether a particular species is pelagic or demersal. The species-specific temperature tolerance range is estimated from empirical studies. If the current month's temperature is outside the temperature tolerance range, the velocity and the migrating fraction of the biomass at the grid point are calculated, the migrating biomass is computed using equations (1) through (7) and, finally, the migrated biomass is added to the nonmigrating biomass at each grid point.

The calculations of migrating fraction and velocity include two types of temperature dependence. First, the difference between the current month's temperature and the species-specific lower tolerance limit (if the temperature is below the minimum) or the upper tolerance limit (if the temperature is above the maximum) is used. Second, the change in temperature from the previous month (i.e., the temporal temperature gradient) is included. Bering Sea temperatures are generally lower than the maximum allowable species-specific temperatures; thus no migrations due to high temperature occur in this area. However, simulated Bering Sea migrations away from cold areas, or away from areas with large month-to-month fluctuations in temperature do occur.

SIMULATION RESULTS

The direct effects of realistic temperature fluctuations on the Bering Sea ecosystem were examined by comparing spatial changes in temperature-induced migration patterns between the cold year (1976) and the warm year (1981). Only a fraction of the biomass at each grid point migrates and, since month-end biomass is a function of several model processes, overall biomass distributions caused by temperature fluctuations are subtle and changes in migration patterns are difficult to determine from biomass distributions alone. However, the change in biomass due to temperature-induced migration (i.e., biomass before migration minus biomass after migration) at each monthly model time step shows distinct changes in migration patterns caused by changes in temperature among the three years.

The analyzed monthly surface and bottom temperature fields for 1976 (cold year) and 1981 (warm year) are presented in the appendices. Even in the cold year, surface temperatures from August, the initial model month, through November are fairly mild, and simulated autumn temperature-induced migrations of pelagic species groups were very similar in the cold and warm years. The bottom temperatures during autumn, however, show a much larger spatial extent of very cold (<0° C) water over the shelf during the cold year than during the warm year. The change in biomass due to temperature-induced migrations of yellowfin, *Limanda aspera*, and rock sole, *Lepidopsetta bilineata*, a demersal species group which uses the bottom temperature field in the model, are shown in Figure 13 for September, October, and November for both the cold and warm year runs. Regions of negative biomass change ("out-migration" regions, where there was a net loss of biomass over the month) are shaded. Out-migrations of yellowfin and rock sole were restricted to the region of the persistent

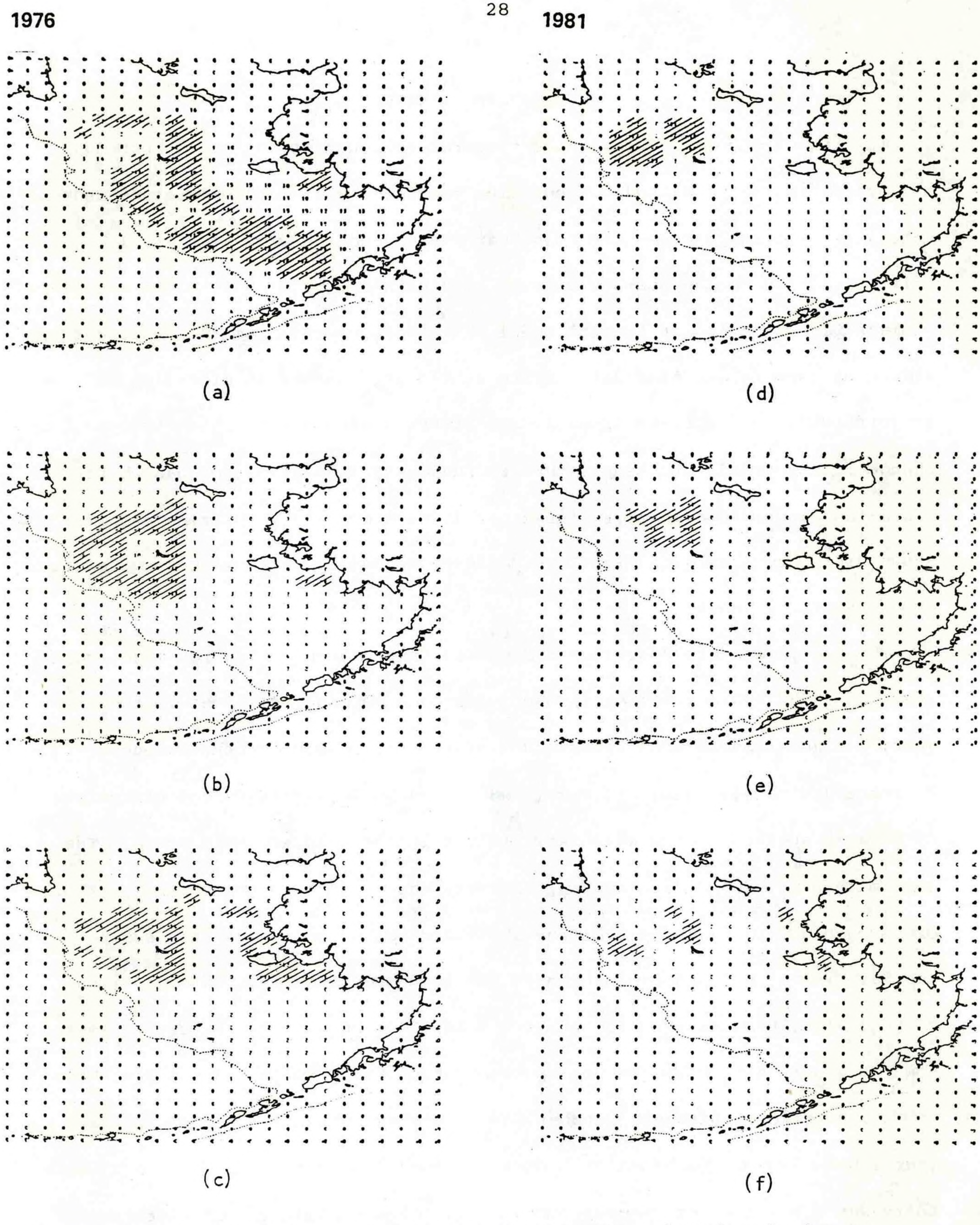

Figure 13.--Simulated change of biomass of yellowfin and rock sole due to temperature-induced migrations during September (top panel), October (center), and November (bottom) of 1976 (cold year) and 1981 (warm year).

cold core of water (see Section 2) until November of the warm year. During the early autumn of the cold year (Fig. 13a) the colder bottom water over the shelf caused a broader extent of outmigrations. These minor migration pattern differences between the warm and cold year runs decrease by January and migration patterns appear similar through November (Figs. 13c and 13d). From December through February, the winter surface and bottom temperature patterns are set up. Surface temperatures are very low, even in the warm year, and ice covers much of the Bering Sea. Bottom temperature patterns during the cold and warm years are nearly identical during this period. Temperature-induced migrations for both pelagic and demersal species groups are minimal during this "rest season" when winter distributions exist.

The most dramatic pattern changes occur during the spring migration period. Spring migrations of yellowfin and rock sole (demersal) and of walleye pollock, Theragra chalcogramma (pelagic) are inshore into Bristol Bay and then north along the Alaskan coast. The change of biomass due to temperature-induced migrations during April, May, and June is presented in Figure 14 (yellowfin and rock sole) and Figure 15 (pollock). During the warm year, 1981, simulated migration into Bristol Bay began in April (Figs. 14d, 15d). During May, migration continued northward along the coast and by June summer biomass distributions were established and inshore migrations were minimal. The simulated results from the cold year, 1976, show the same inshore migration, but the migration into Bristol Bay occurs at a 2-month lag. Northward migration along the coast is not evident in the cold year until June. Model simulations using the mean temperature fields showed migration patterns with characteristics of both extremes: minimal migration into Bristol Bay began in April and northward migration along the coast continued in June.

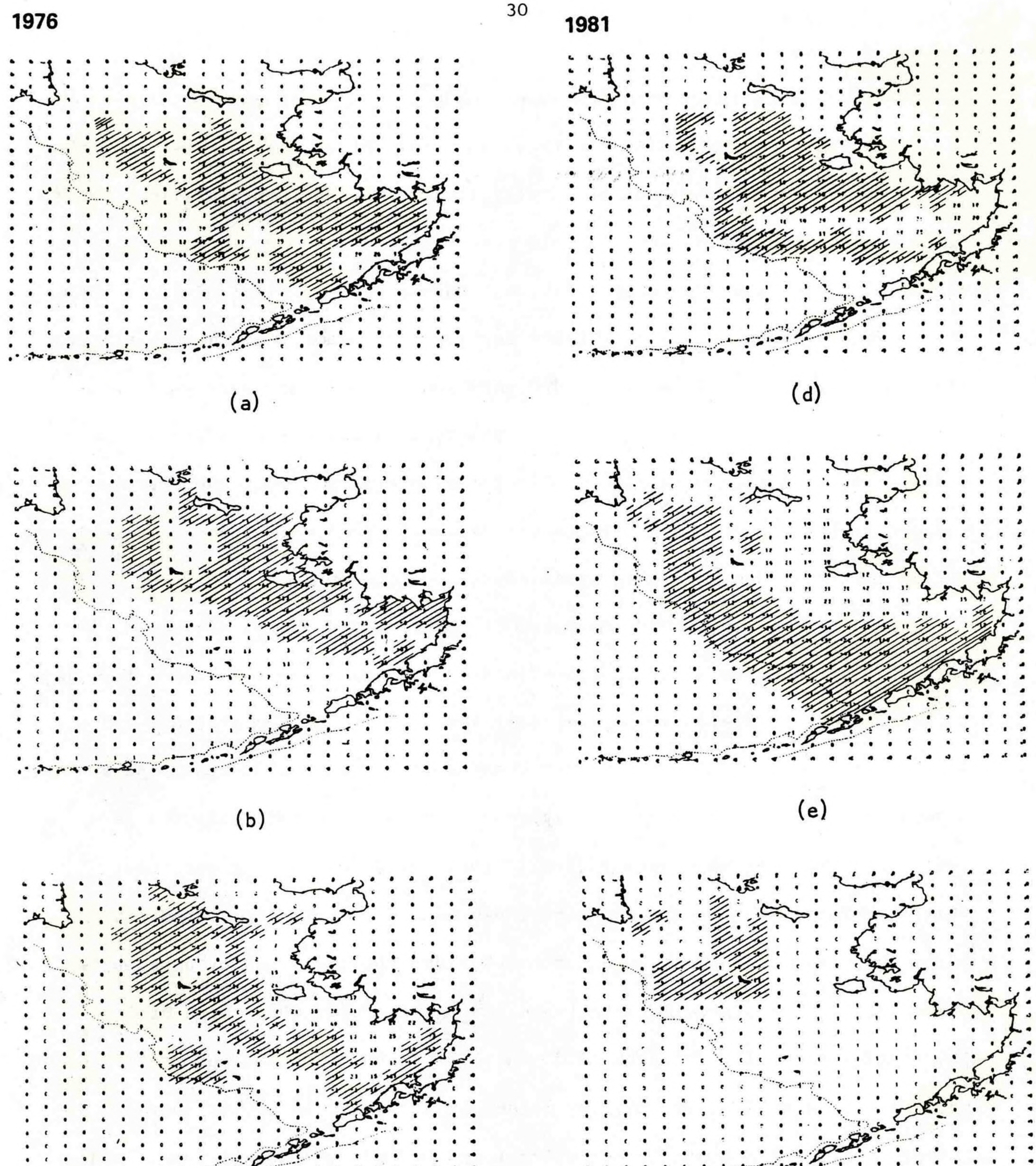

Figure 14.--Simulated change of biomass of yellowfin and rock sole due to temperature-induced migrations during April (top panel), May (center) and June (bottom) of 1976 (cold year) and 1981 (warm year).

1976

1981

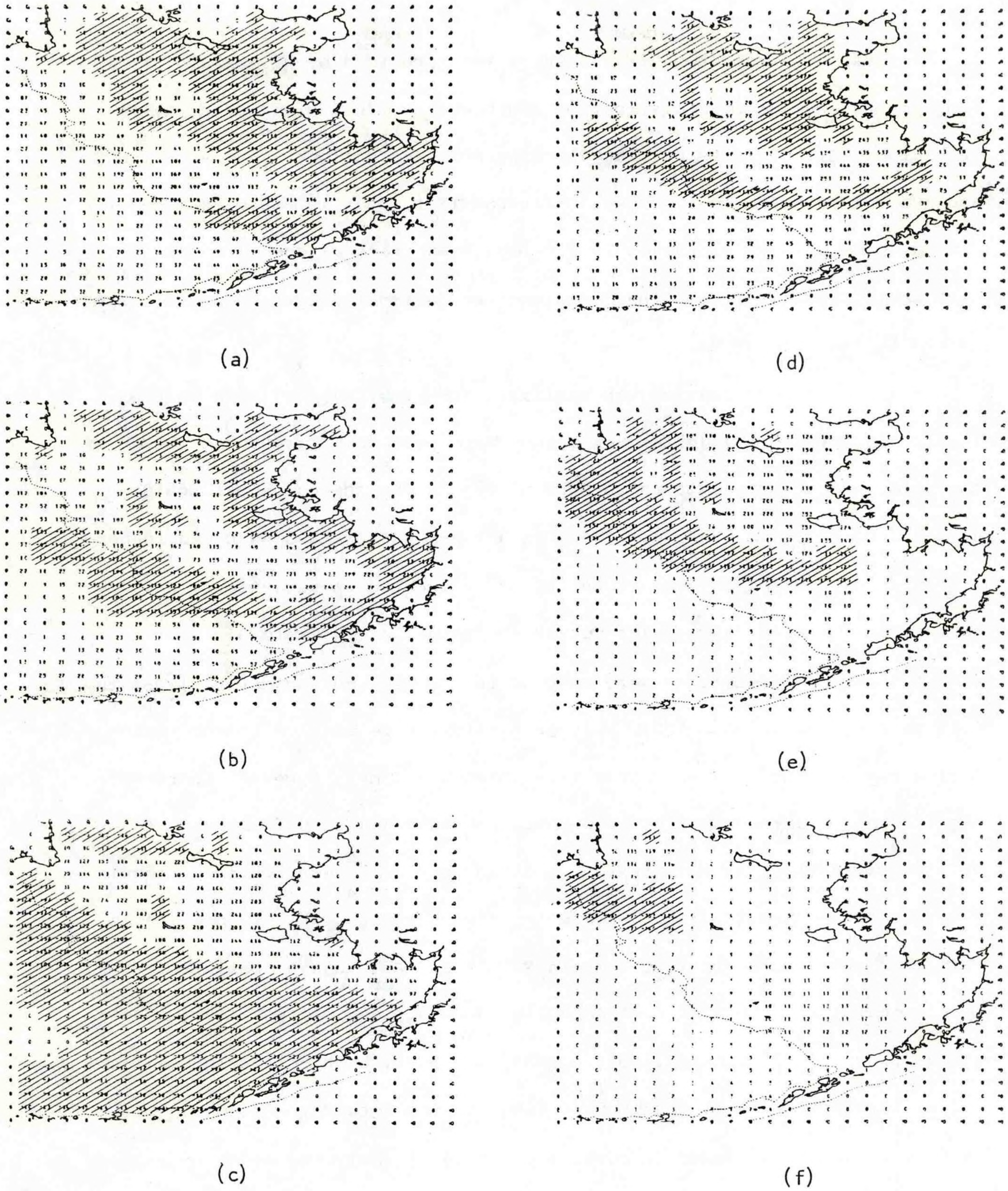

Figure 15.--Simulated change of biomass of walleye pollock due to temperature-induced migrations during April (top panel), May (center) and June (bottom) of 1976 (cold year) and 1981 (warm year).

Observations from groundfish surveys were provided by R. Bakkala of the Resource Assessment and Conservation Engineering (RACE) Division at NWAFC (Bakkala 1983). Results of the yellowfin sole and pollock surveys from May and June of 1976 and 1981, shown in Figures 16 through 19, were examined for similarities with model results. Stations with trace catches are designated with solid triangles; all other stations are designated by "+", and biomass caught is given in kg/ha.

If the simulated results are realistic, one would expect more catches inshore in Bristol Bay during May of the warm year than were found in May of the cold year. Also, catches in Bristol Bay during the cold year would be expected to increase in June. The area between 56°43'N and 59°N and inshore of 166°42'W (Bristol Bay and vicinity) is delineated in each figure and catches in the area during each survey are tabulated in Table 3.

A total of 40 stations were sampled in the area during May of 1976, the cold year (Figs. 16a and 17a); only 24 stations were sampled in the region during May of 1981, the warm year (Figs. 16b and 17b). However, there were significantly more catches of both yellowfin sole and of pollock within Bristol Bay during the warm year than during the cold year, which is consistent with simulated results. Yellowfin sole catches in June of the cold year (Fig. 18a) were more numerous than in May (Fig. 16b), again consistent with model results. Catches of pollock during June of the cold year (Fig. 19a), however, were still minimal. During the warm year, both yellowfin sole and and walleye pollock were caught in Bristol Bay in both May and June. Pollock catches actually decreased in June, suggesting an early abundance of pollock in Bristol Bay during May of the warm year.

Table 3.--Results of simulation model and from groundfish surveys of walleye pollock and yellowfin sole during 1976 (cold year) and 1981 (warm year) in the region delineated in Figures 15 and 16.

			Survey Results 1/							
			Yellowfin Sole				Walleye Pollock			
Year	Month	Simulation Model Results	Stations sampled	Stations with catches	Average biomass	Maximum biomass	Stations sampled	Stations with catches	Average biomass	Maximum biomass
1976 (cold year)	May	Begin spring migration into Bristol Bay	40	36	10.5	46	40	0	0	trace
	June	Continue inshore migration in the area north of Bristol Bay along the Alaskan coast	43	43	81.8	1,335	43	5	0.8	16
1981 (warm year)	May	Continue inshore migration in the area north of Bristol Bay along the Alaskan coast	24	24	116.0	284	24	24	63.1	695
	June	Summer distribution patterns set	39	39	148.4	395	39	24	29.5	419

1/ All numbers refer to the area north of 56°43'N and inshore of 166°42'W. Stations with no catches are denoted by "+" without catch numbers. Stations with trace catches are denoted by "Δ". Biomass values are in kg/ha.

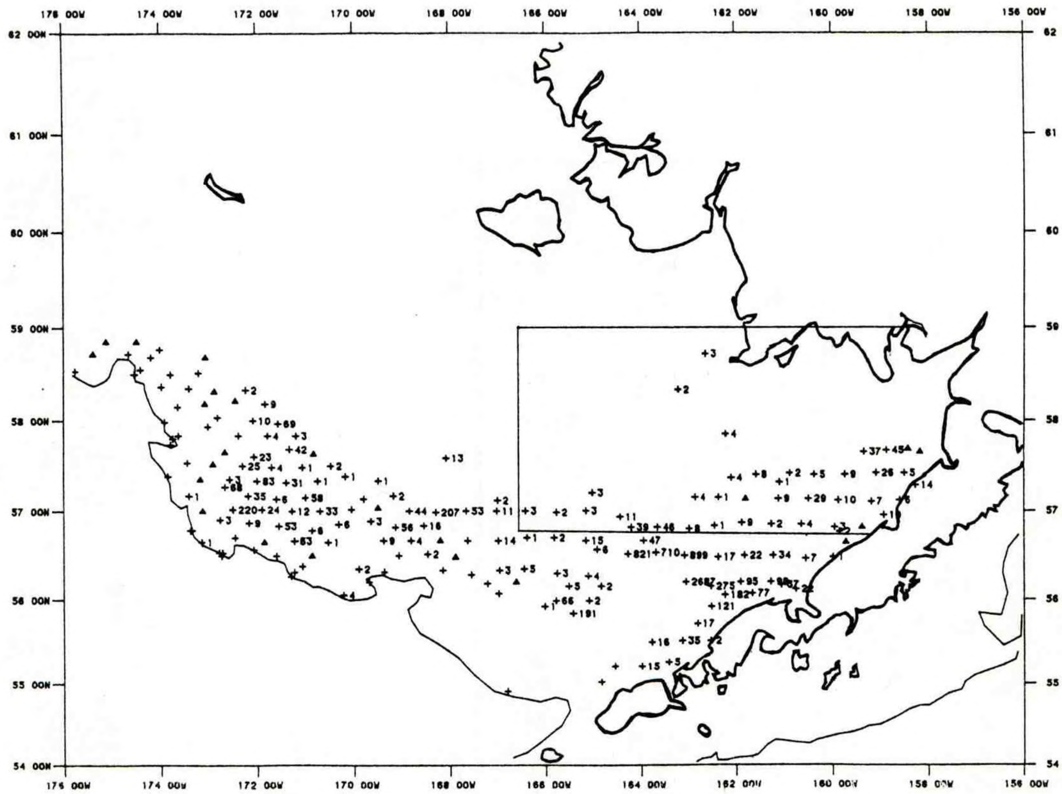

Figure 16a.--Catches of yellowfin sole, in kg/ha, during the May 1976 (cold year) groundfish survey.

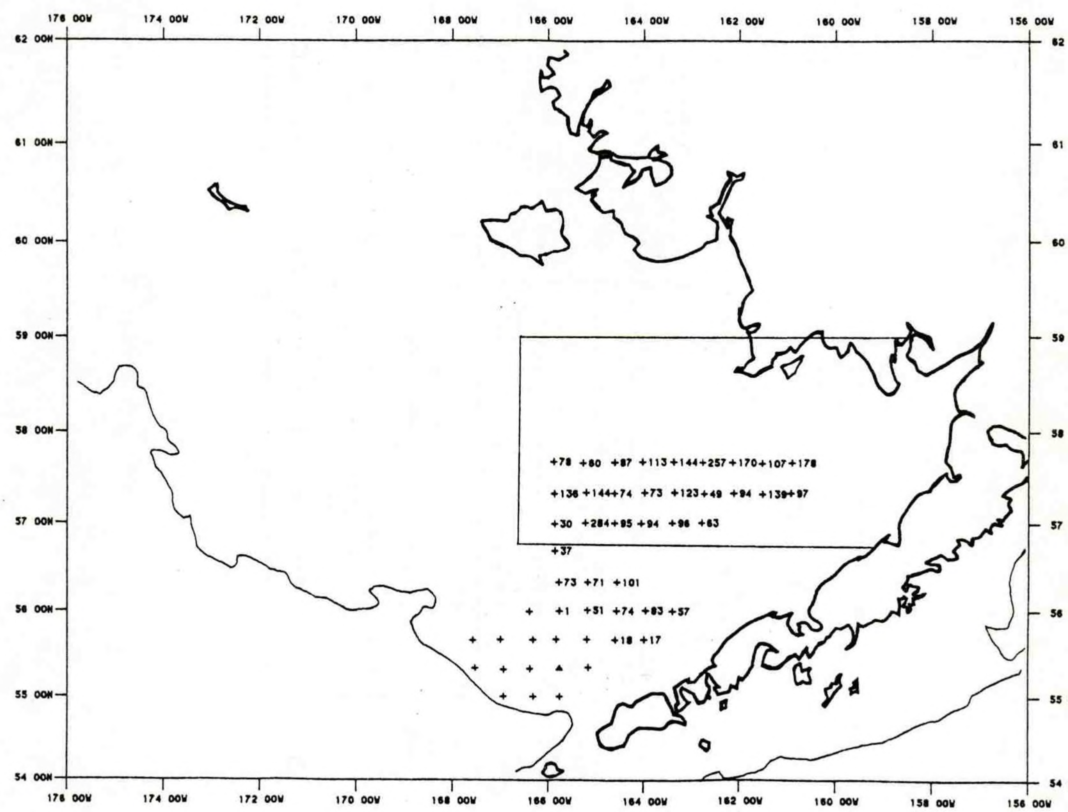

Figure 16b.--Catches of yellowfin sole, in kg/ha, during the May 1981 (warm year) groundfish survey.

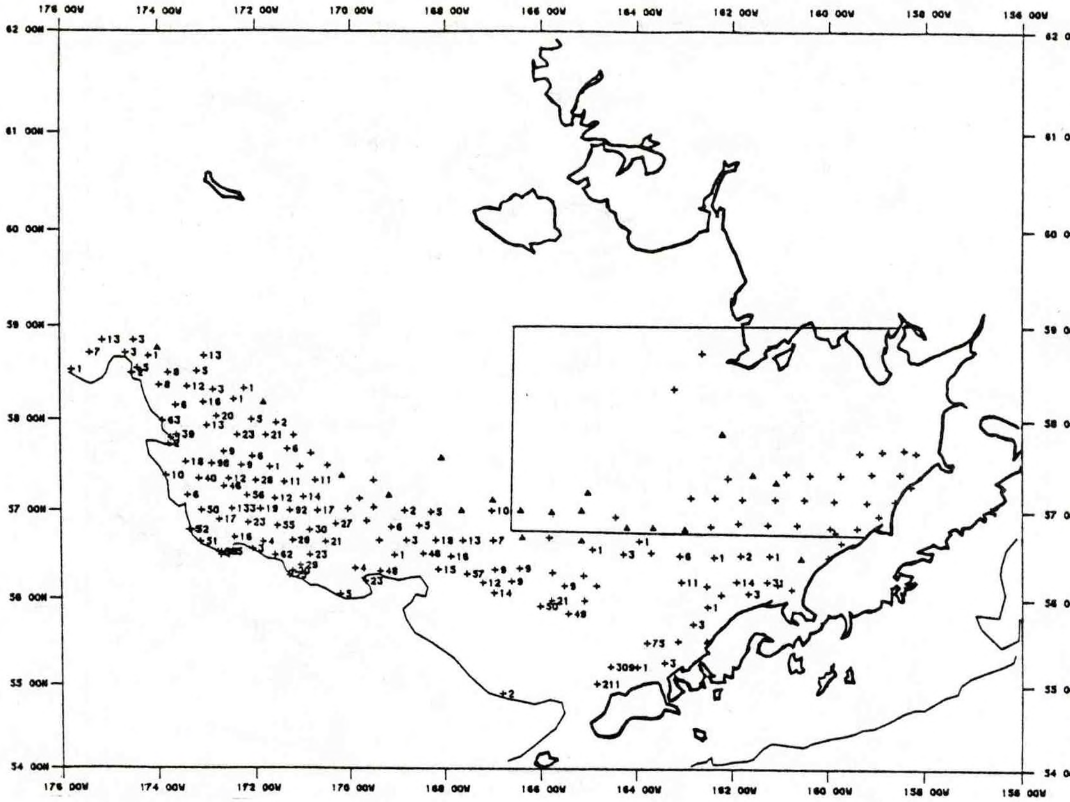

Figure 17a.--Catches of walleye pollock, in kg/ha, during the May 1976 (cold year) groundfish survey.

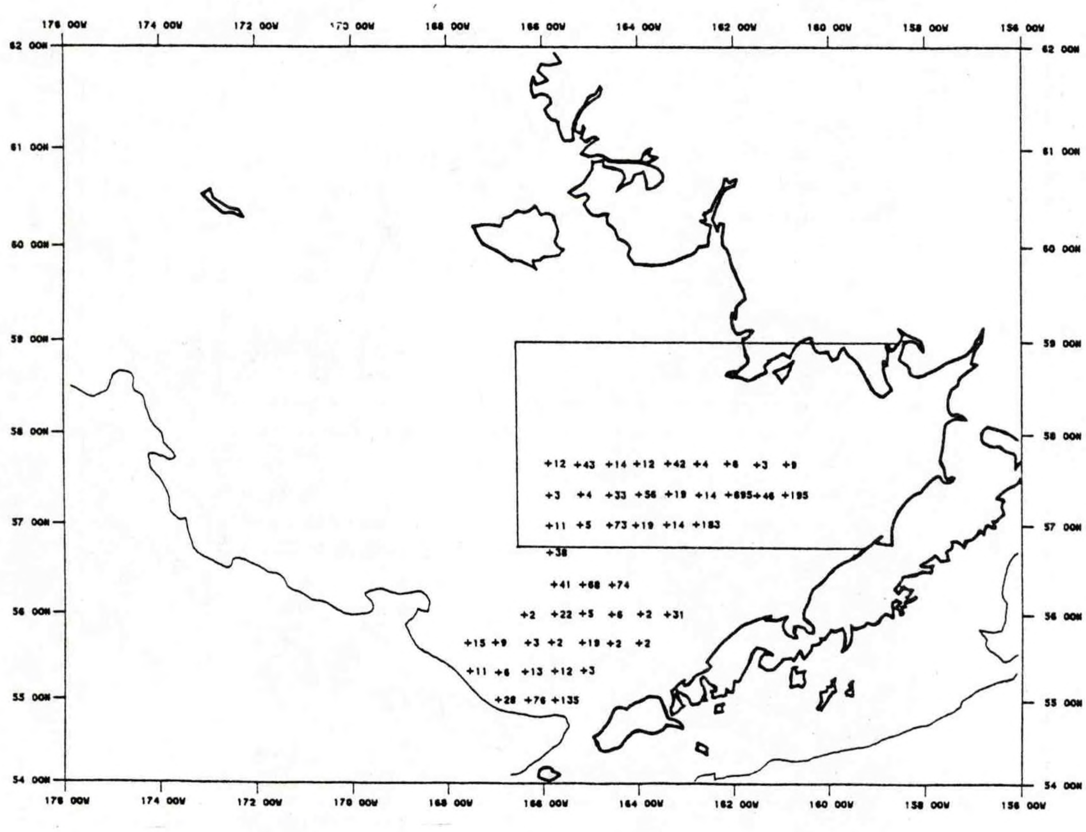

Figure 17b.--Catches of walleye pollock, in kg/ha, during the May 1981 (warm year) groundfish survey.

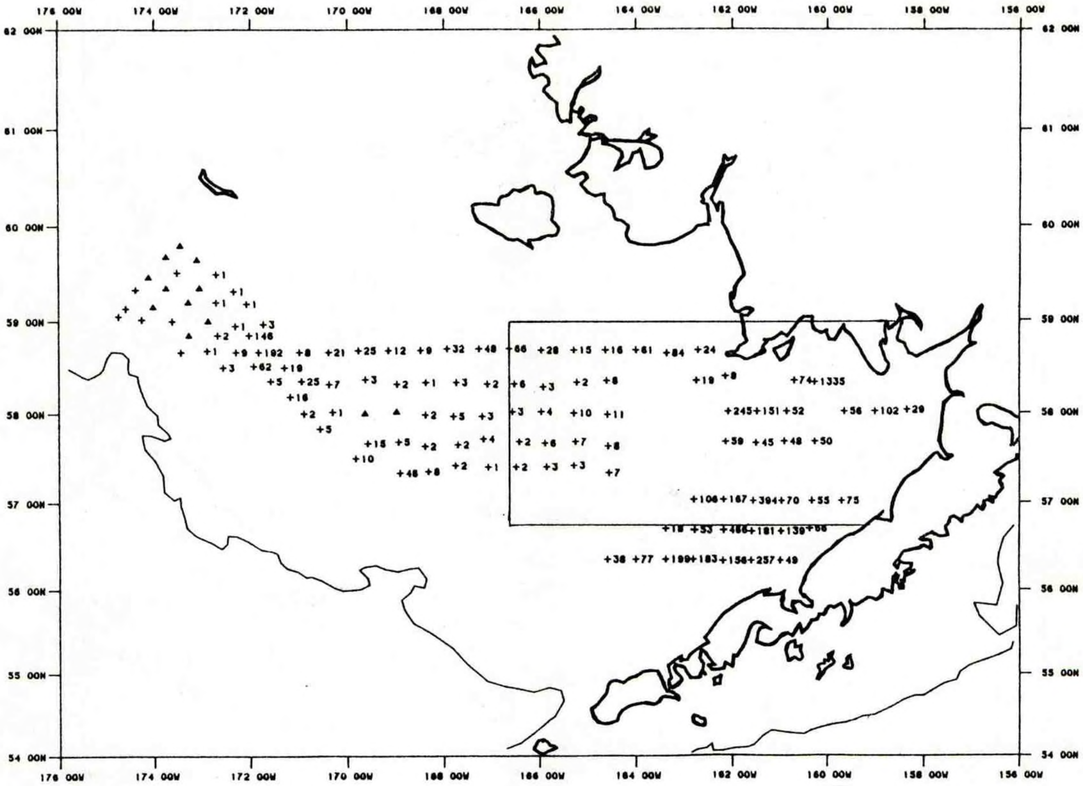

Figure 18a.--Catches of yellowfin sole, in kg/ha, during the June 1976 (cold year) groundfish survey.

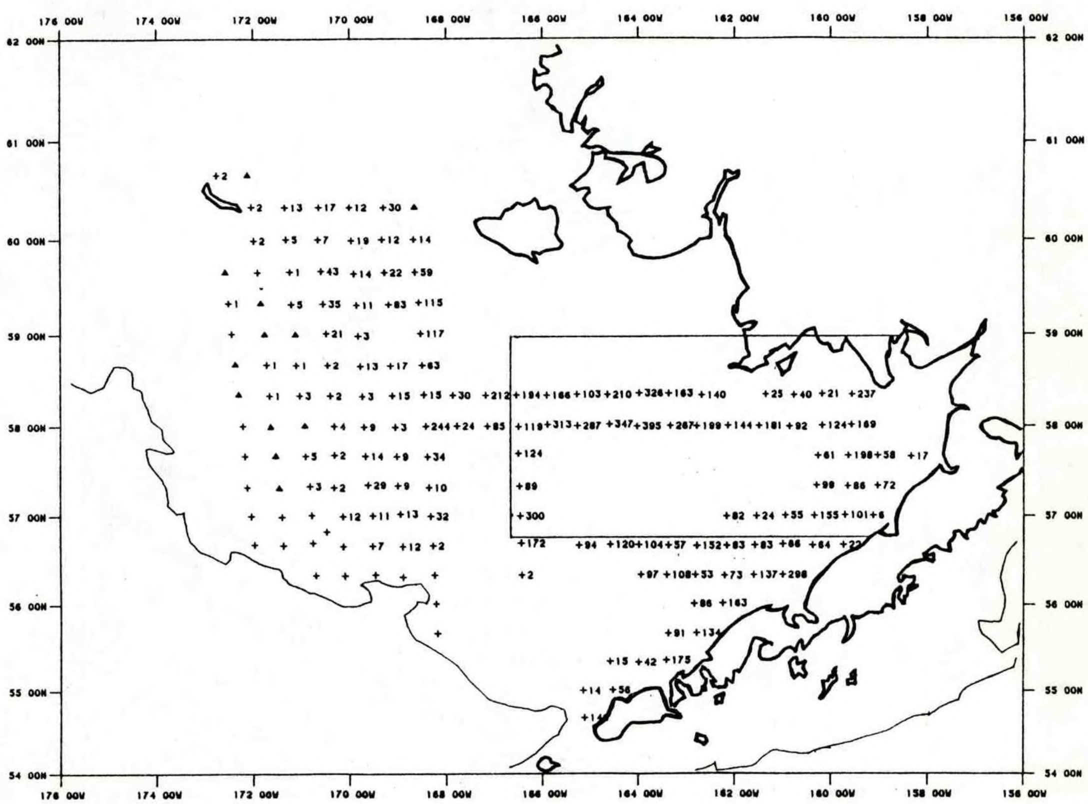

Figure 18b.--Catches of yellowfin sole, in kg/ha, during the June 1981 (warm year) groundfish survey.

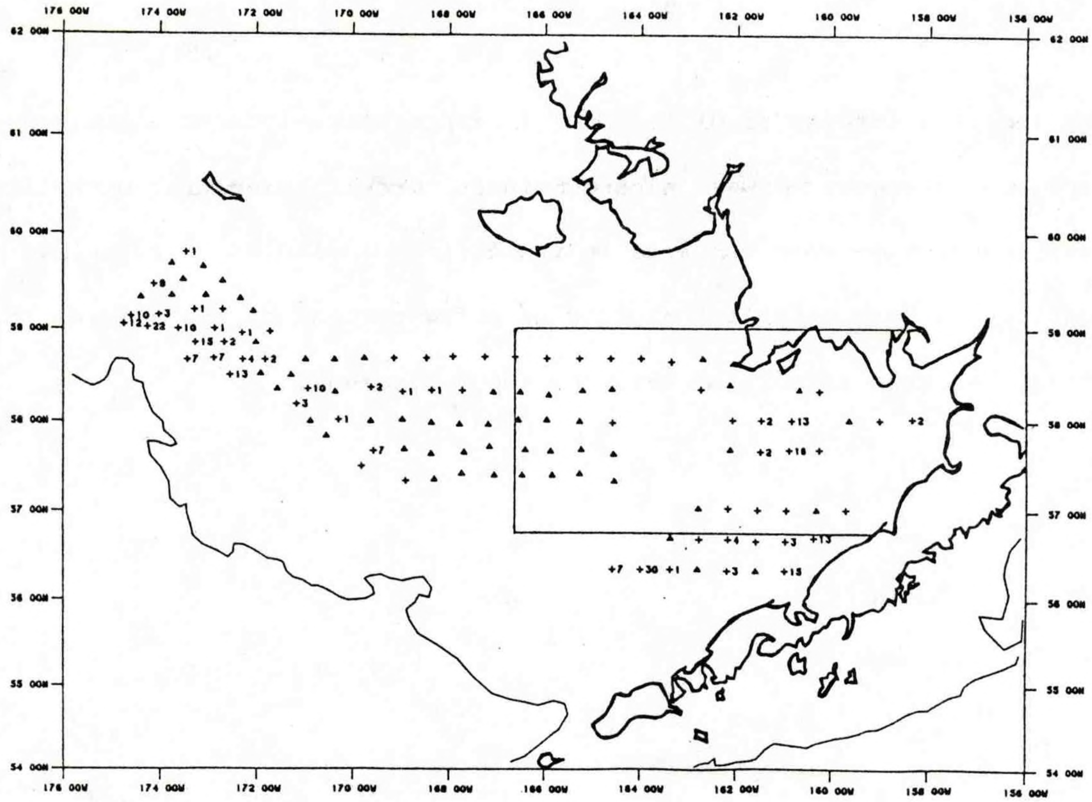

Figure 19a.--Catches of walleye pollock, in kg/ha, during the June 1976 (cold year) groundfish survey.

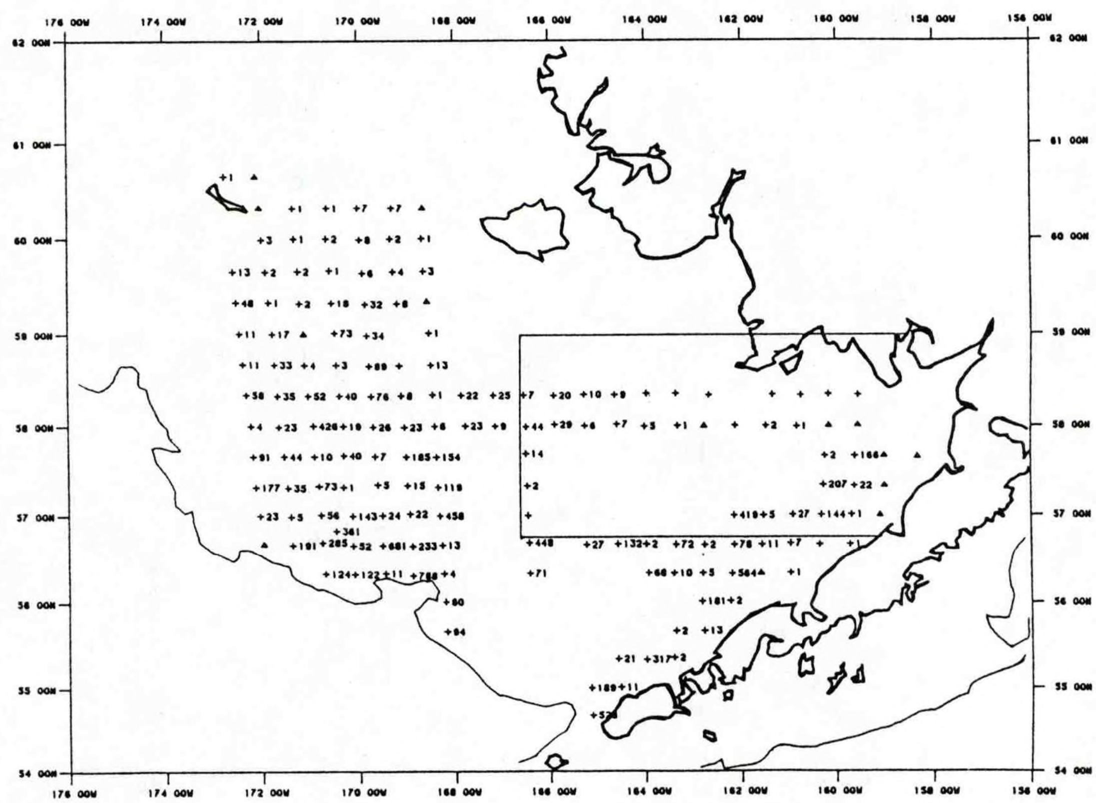

Figure 19b.--Catches of walleye pollock, in kg/ha, during the June 1981 (warm year) groundfish survey.

The indirect effects of differences in temperature-induced migration patterns on the ecosystem were also examined. Growth, predation mortality and prey consumption were compared in the different simulation runs, but maximum changes were only on the order of a few percent of the biomass (i.e., less than the error associated with the input biomass).

CONCLUSIONS

The most significant changes in simulated migration patterns between warm (1981) and cold (1976) years for yellowfin sole and walleye pollock occurred during spring, when inshore migrations into Bristol Bay during the cold year lagged those of the warm year by two months. Available field survey data for May of the same years are consistent with simulated results: catches of both pollock and yellowfin sole within Bristol Bay during May were significantly greater in 1981 than in 1976. Yellowfin sole catches in Bristol Bay during the cold year increased in June, which again is consistent with the model results. Pollock catches during June of the cold year, however, were still minimal. During the warm year, pollock abundance in Bristol Bay appeared to peak in May. These simulated changes in spring migration patterns caused by interannual temperature fluctuations, if realistic, would be of considerable importance to fisheries management programs.

This study has been a preliminary effort to ascertain the effects of the environment on a marine ecosystem. The only temperature effects studied in detail were changes in migration patterns. Only two model species groups were studied and only 2 years of extreme temperature data were input to the model. Additional comparisons to survey data would be useful; however, field surveys in the eastern Bering Sea have been routinely performed only during the past decade, and differences in sampling gear configuration between surveys can reduce our ability to compare interannual survey results. If surveys continue over time, if the frequency of observations is increased, and if simultaneous temperature and biological data are obtained, the dynamics of the model can be further tested. In addition, other components of the ecosystems which may be affected by temperature or by changes in migration patterns (e.g., fluctuations in fishing effort and changes in the timing of spawning and possible effects) can be studied in the future with ecosystem simulation models.

REFERENCES

BAKKALA, R. G.

1983. Research and commercial fisheries data bases for eastern Bering Sea groundfish. Unpubl. manuscr., 27 p. Northwest and Alaska Fish. Cent., Natl. Mar. Fish. Serv., NOAA, 2725 Montlake Blvd. E., Seattle, WA 98112.

GALLAGHER, A. F., Jr.

1983. Biomass-based fisheries ecosystem simulations of the North Pacific--general overview of the DYNUMES and SKEBUB simulation models. NWAFC Processed Rep. 83-10, 34 p. Northwest and Alaska Fish. Cent., Natl. Mar. Fish. Serv., NOAA, 2725 Montlake Blvd. E., Seattle, WA 98112.

INGRAHAM, W. J., Jr.

1981a. Temperature and salinity observations at surface and near bottom over the eastern Bering Sea shelf, averaged by 1° x 1/2° squares. NWAFC Processed Rep. 81-09, 52 p. Northwest and Alaska Fish. Cent., Natl. Mar. Fish. Serv., NOAA, 2725 Montlake Blvd. E., Seattle, WA 98112.

INGRAHAM, W. J. Jr.

1981b. Shelf environment. In D. W. Hood and J. A. Calder (editors), The eastern Bering Sea shelf: oceanography and resources, Vol. 1., p. 455-470. U.S. Gov. Print. Off., Washington, D.C.

INGRAHAM, W. J., Jr.

1983. Temperature anomalies in the eastern Bering Sea 1953-82 for the DYNUMES 24x24 ecosystem model grid. NWAFC Processed Rep. 83-21, 348 p. Northwest and Alaska Fish. Cent., Natl. Mar. Fish. Serv., NOAA, 2725 Montlake Blvd. E., Seattle, WA 98112.

INGRAHAM, W. J., Jr., N. POLA SWAN, Y. LEE, R. MIYAHARA, and M. HAYES.

1983. Processing of FNWC daily sea level pressure data on NWAFC Burroughs 7811. REFM Program Doc. 19, 101 p. Northwest and Alaska Fish. Cent., Natl. Mar. Fish. Serv., NOAA, 2725 Montlake Blvd. E., Seattle, WA 98112.

LAEVASTU, T.

1976. Predicting pollution dispersal with Hansen's hydrodynamical numerical models. In C. I. Bretschneider (editor), Topics in ocean engineering, Vol. 3, p. 59-69. Gulf Pub. Co., Houston, TX.

LAEVASTU, T.

In Press. The effects of temperature anomalies on the fluctuations of fish stocks. Rapp. P.-V., Reun. Cons. Int. Explor. Mer.

LAEVASTU, T., J. DUNN, and F. FAVORITE.

1976. Consumption of copepods and euphausids in the eastern Bering Sea as revealed by a numerical ecosystem model. Int. Counc. Explor. Sea, Plankton Comm., C.M. 1976/L:34, 10 p.

LAEVASTU, T., and F. FAVORITE.

1978. Numerical evaluation of marine ecosystem. Part II. Dynamical Numerical Marine Ecosystem Model (DYNUMES III) for evaluation of fisheries resources. Processed Rep., 29 p. Northwest and Alaska Fish. Cent., Natl. Mar. Fish. Serv., NOAA, 2725 Montlake Blvd. E., Seattle, WA 98112.

1979. Ecosystem dynamics in the eastern Bering Sea. In Fisheries oceanography - eastern Bering Sea shelf, p. 444-481. NWAFC Processed Rep. 79-20. Northwest and Alaska Fish. Cent., Natl. Mar. Fish. Serv., NOAA, 2725 Montlake Blvd. E., Seattle, WA 98112.

LAEVASTU, T., and H. A. LARKINS.

1981. Marine fisheries ecosystem. Its quantitative evaluation and management. Fishing News Books Ltd., Farnham, Surrey, England, 162 p.

LAEVASTU, T., and R. MARASCO.

1982. Evaluation of fishery resources with ecosystem simulations and quantitative determination of their response to ocean environmental anomalies and fishery. NWAFC Processed Rep. 82-08, 42 p. Northwest and Alaska Fish. Cent., Natl. Mar. Fish. Serv., NOAA, 2725 Montlake Blvd. E., Seattle, WA 98112.

SWAN, N. P.

1983. The role of migrations in ecosystem simulation. NWAFC Processed Rep. 83-08, 29 p. Northwest and Alaska Fish. Cent., Natl. Mar. Fish. Serv., NOAA, 2725 Montlake Blvd. E., Seattle, WA 98112.

APPENDIX A

ANALYZED MONTHLY SURFACE TEMPERATURE

DISTRIBUTION FOR 1976 (COLD YEAR).

Contour interval is 0.5°C.

JANUARY

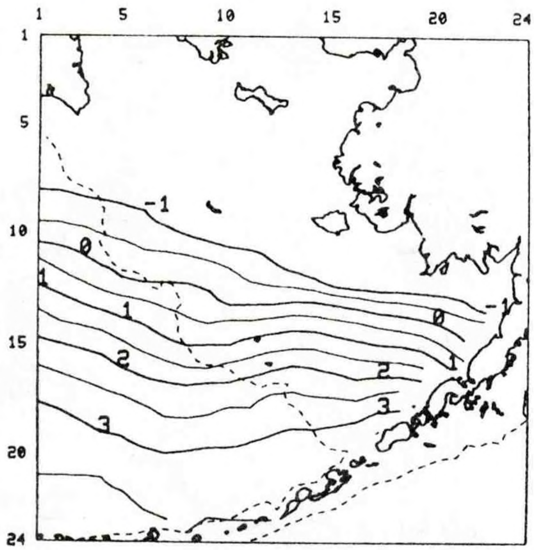

APRIL

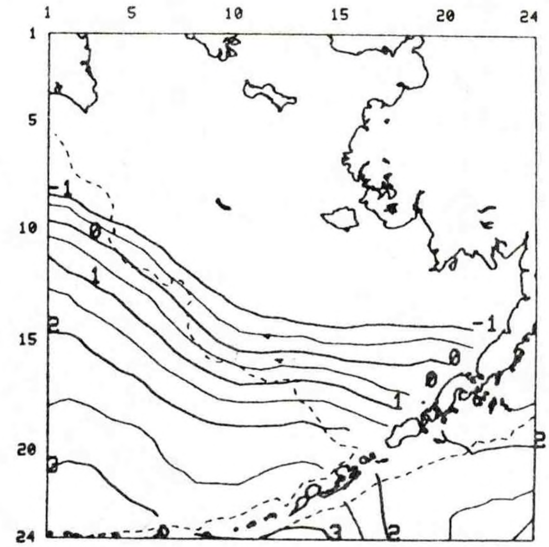

FEBRUARY

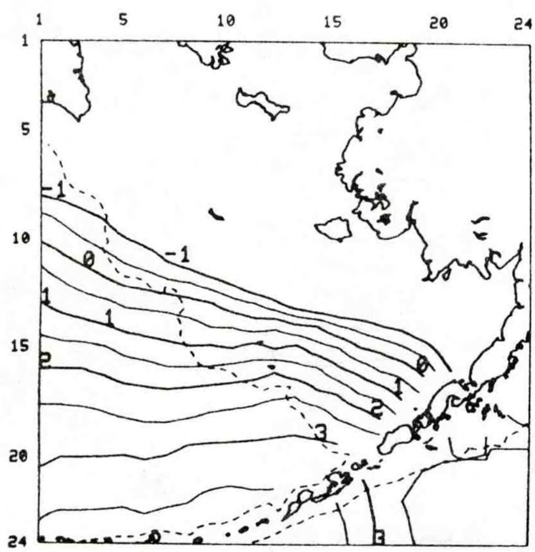

MAY

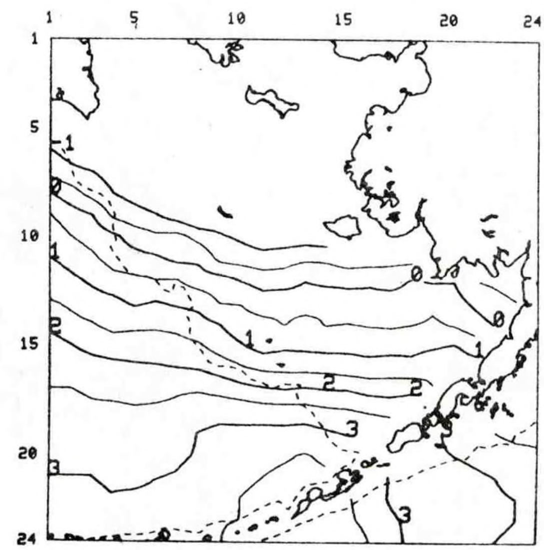

MARCH

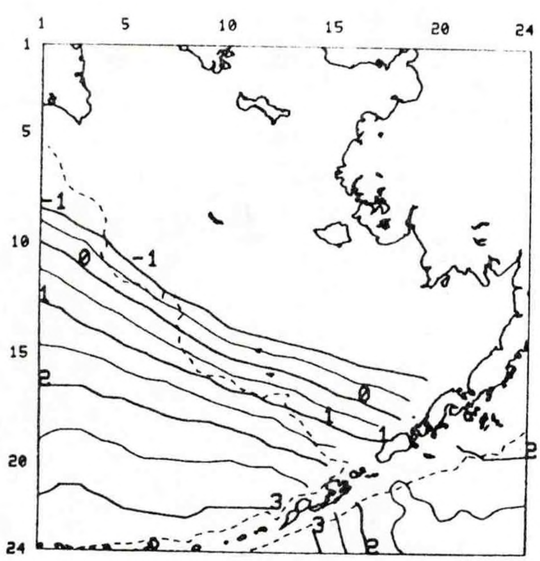

JUNE

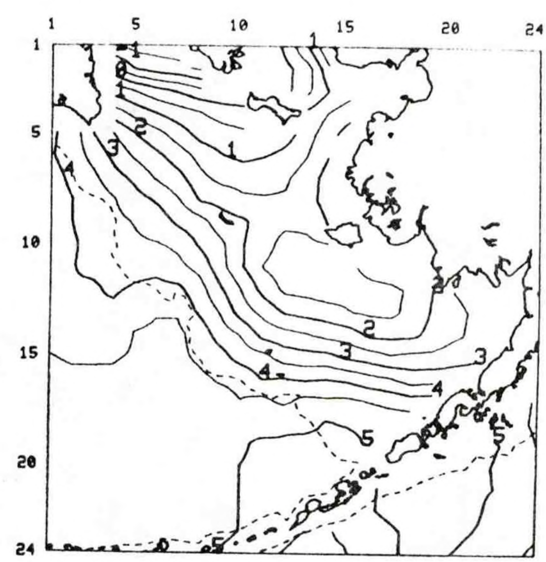

JULY

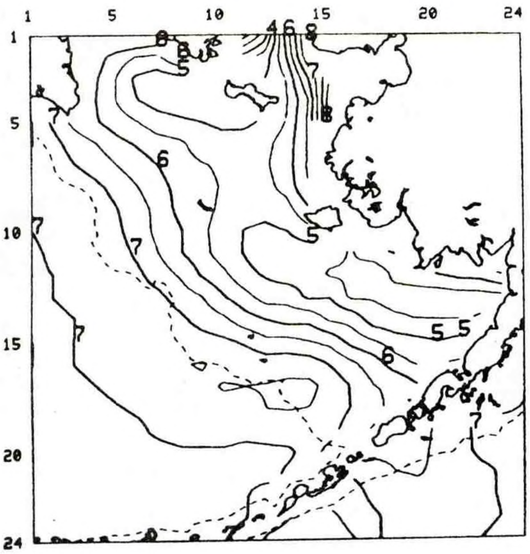

OCTOBER

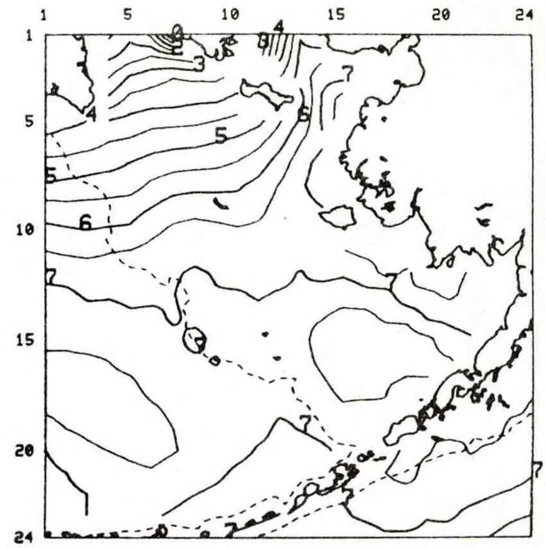

AUGUST

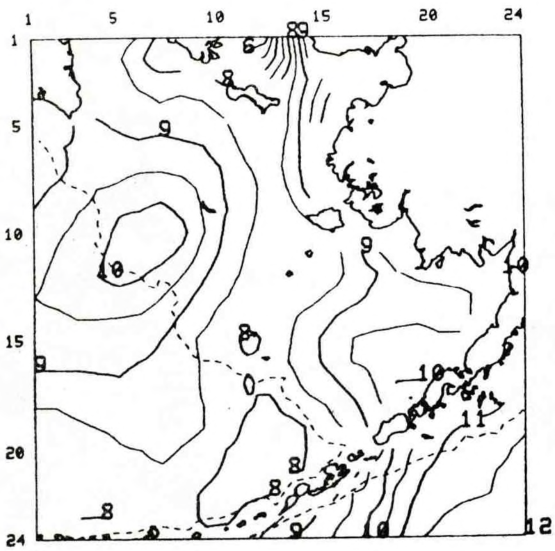

NOVEMBER

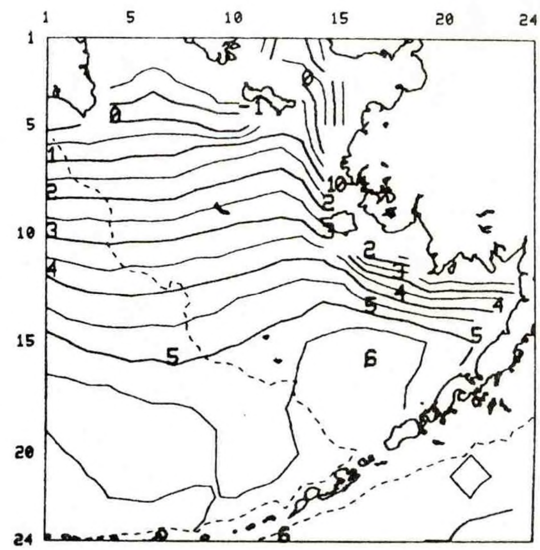

SEPTEMBER

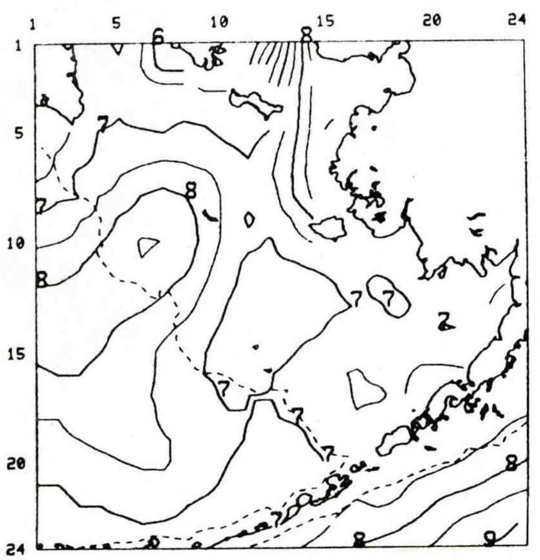

DECEMBER

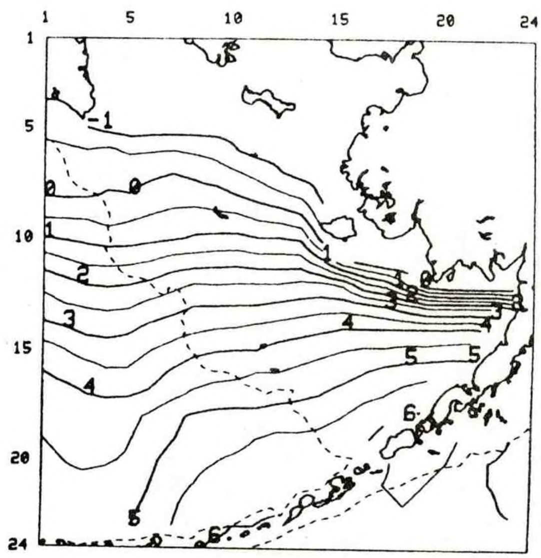

APPENDIX B

ANALYZED MONTHLY BOTTOM TEMPERATURE

DISTRIBUTION FOR 1976 (COLD YEAR).

Contour interval is 1°C.

JANUARY

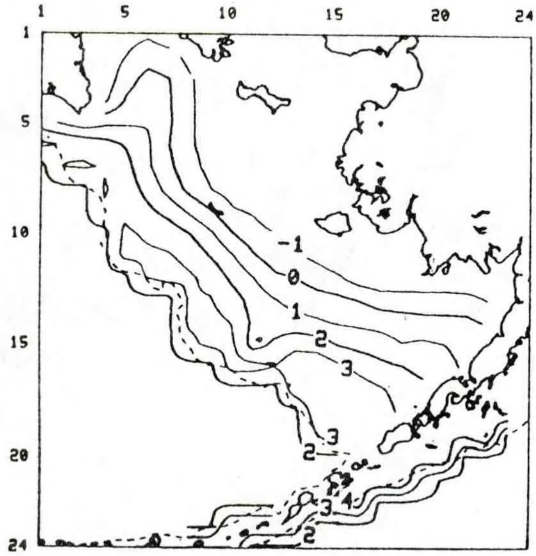

APRIL

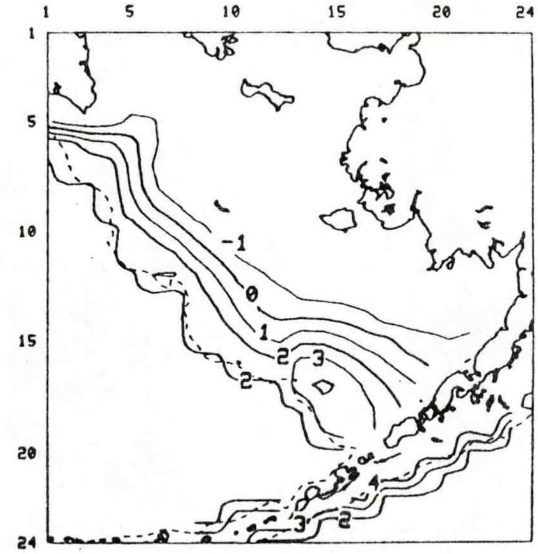

FEBRUARY

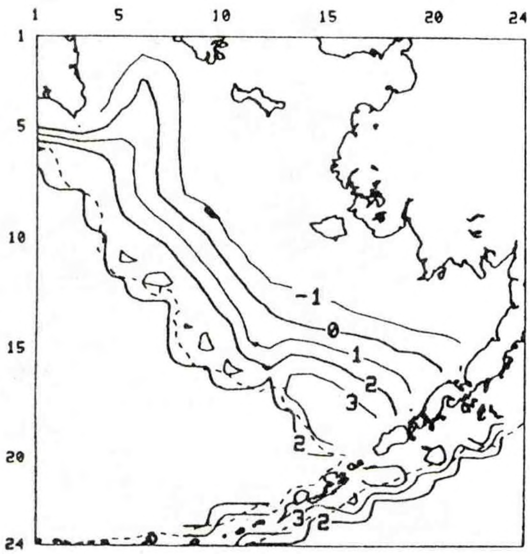

MAY

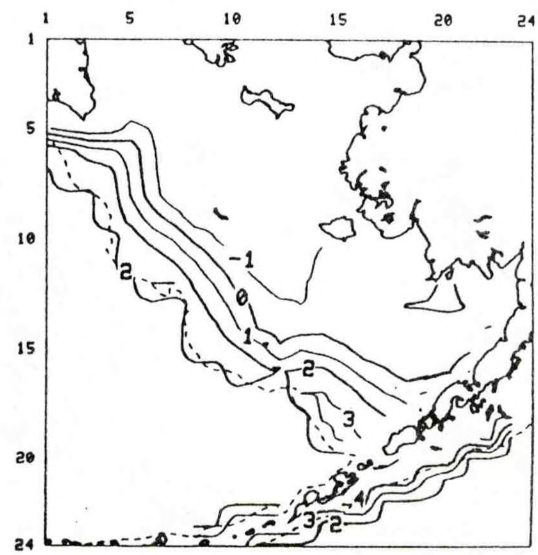

MARCH

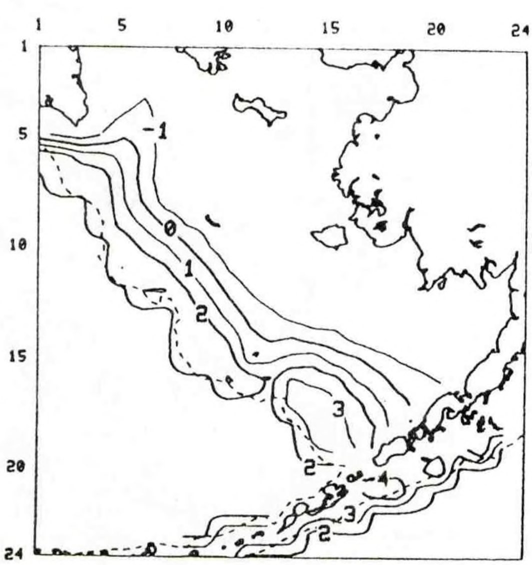

JUNE

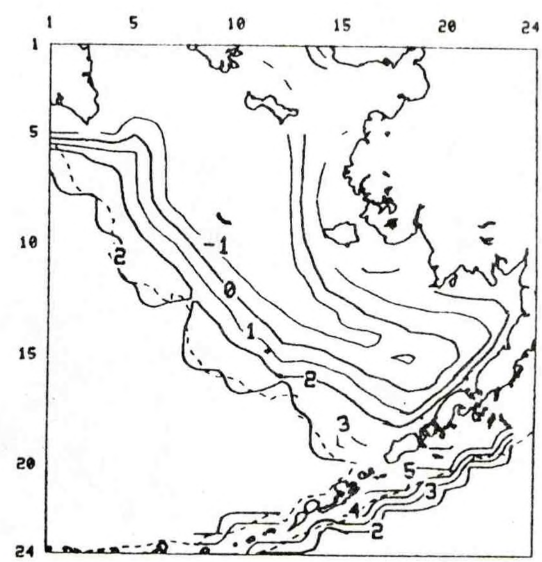

JULY

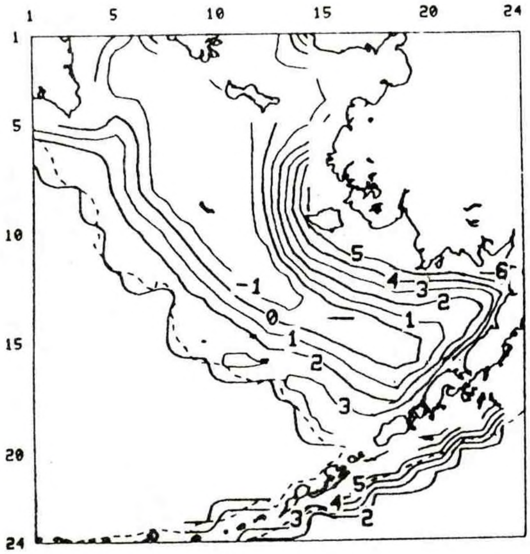

OCTOBER

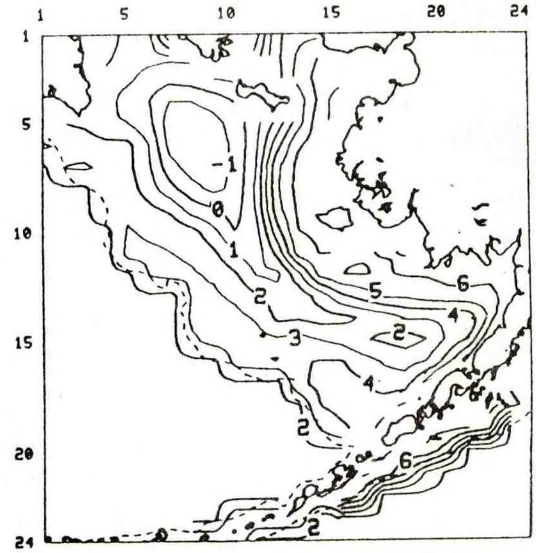

AUGUST

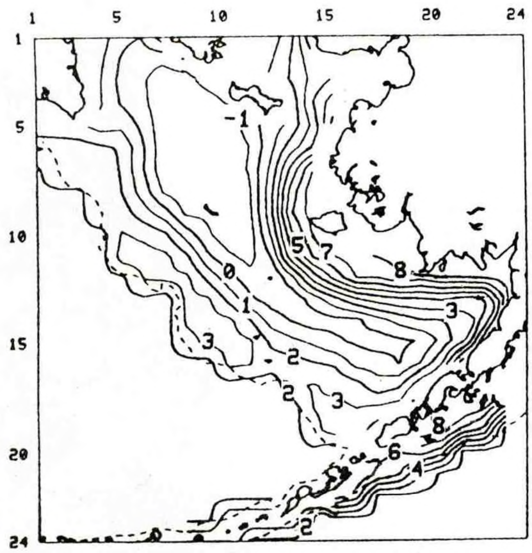

NOVEMBER

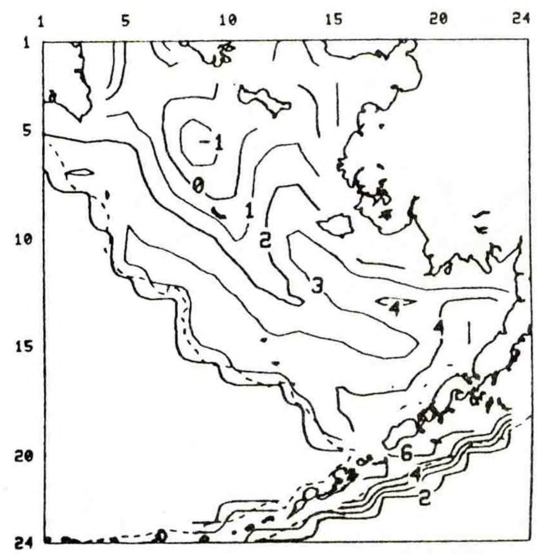

SEPTEMBER

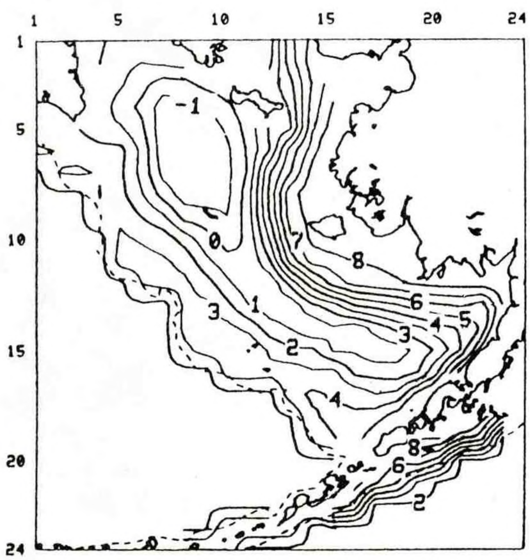

DECEMBER

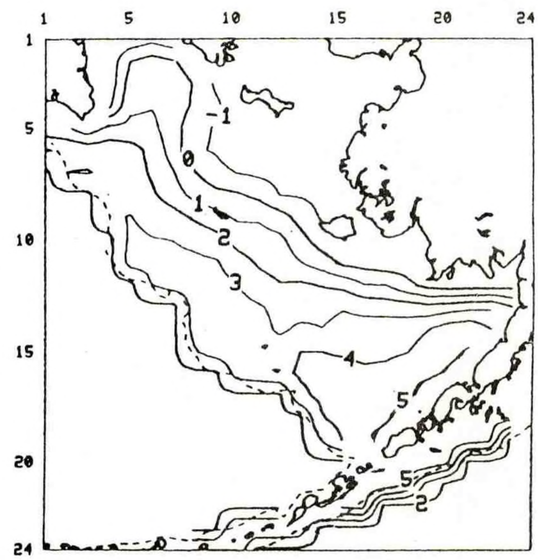

APPENDIX C

ANALYZED MONTHLY SURFACE TEMPERATURE

DISTRIBUTION FOR 1981 (WARM YEAR).

Contour interval is 0.5°C.

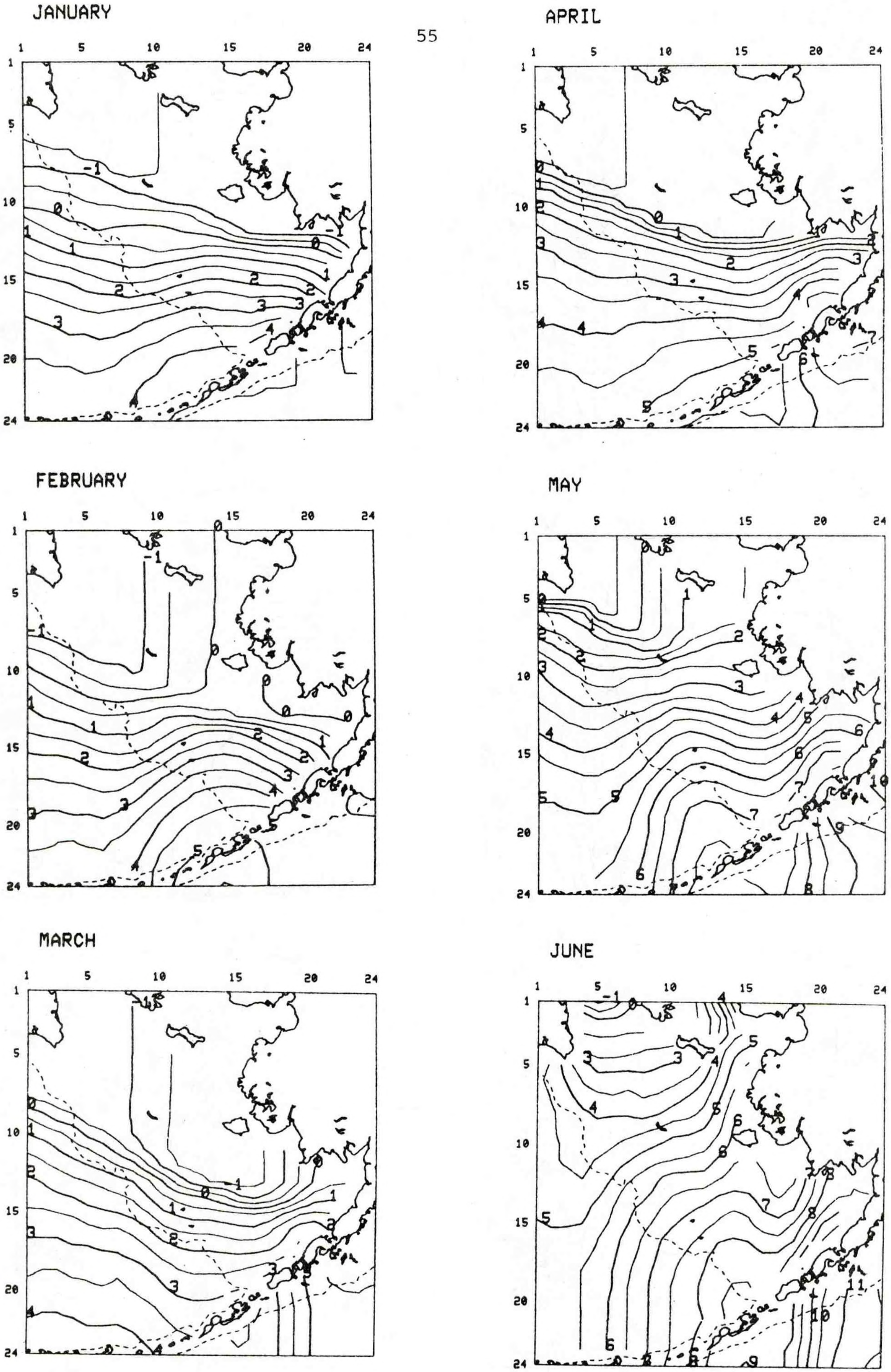
JANUARY
APRIL
FEBRUARY
MAY
MARCH
JUNE

JULY

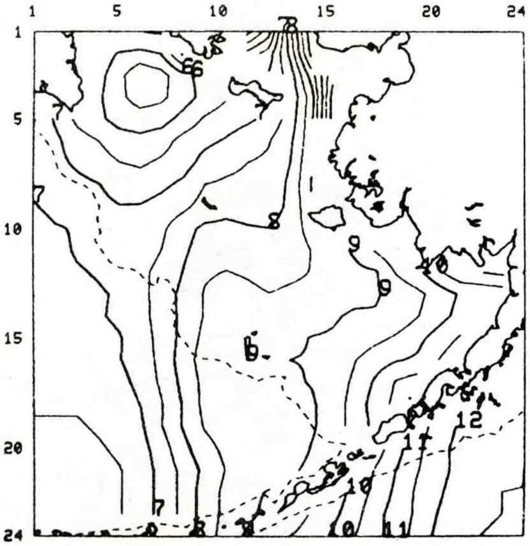

OCTOBER

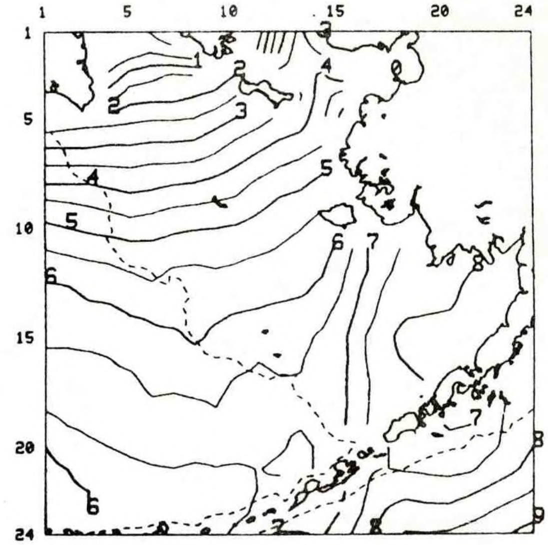

AUGUST

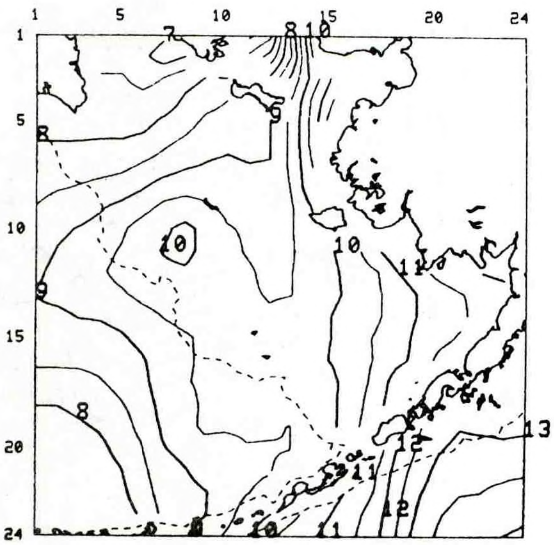

NOVEMBER

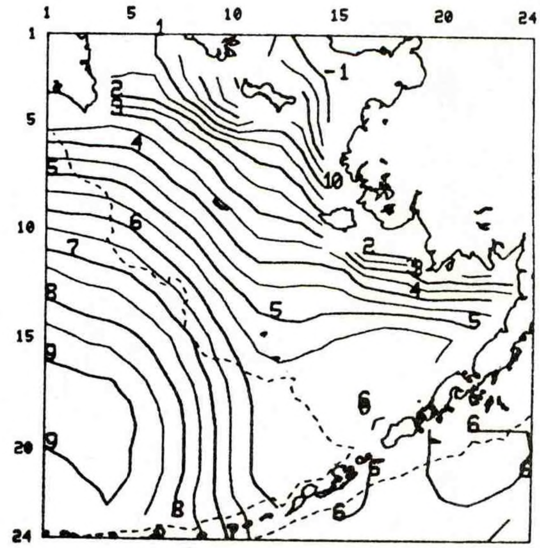

SEPTEMBER

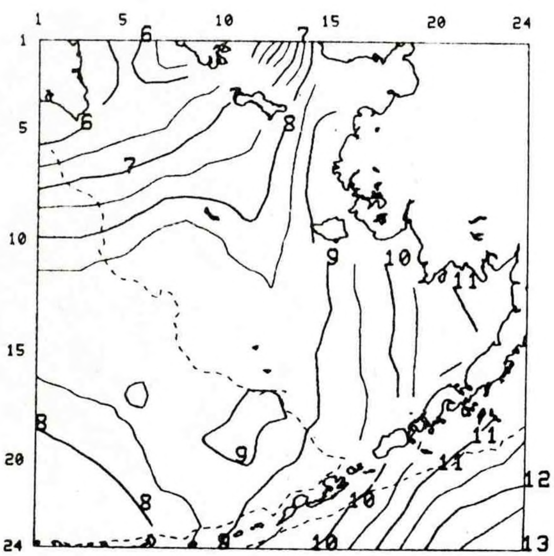

DECEMBER

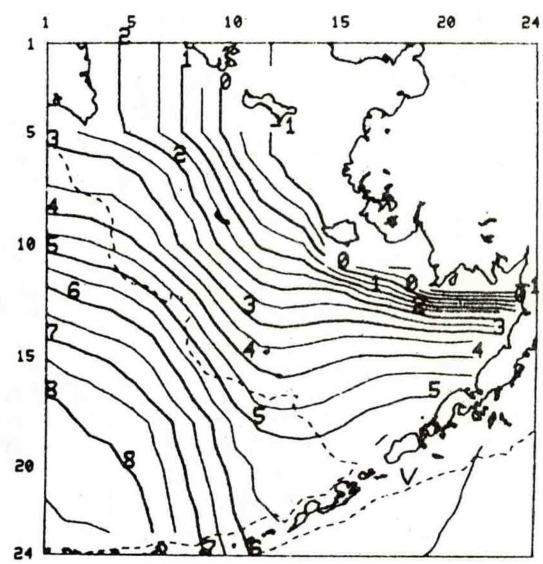

APPENDIX D

ANALYZED MONTHLY BOTTOM TEMPERATURE

DISTRIBUTION FOR 1981 (WARM YEAR).

Contour interval is 1°C.

JULY

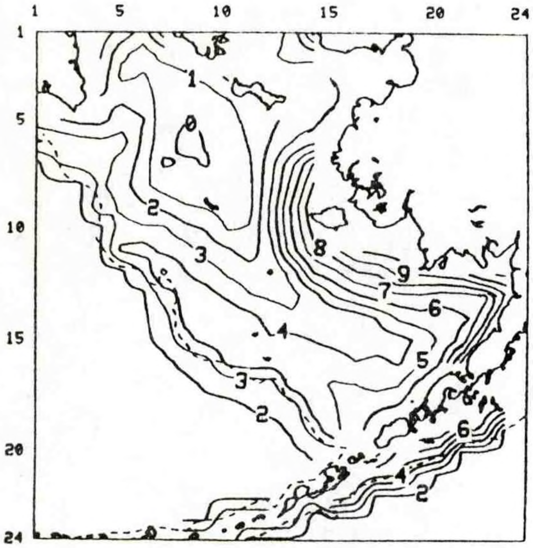

AUGUST

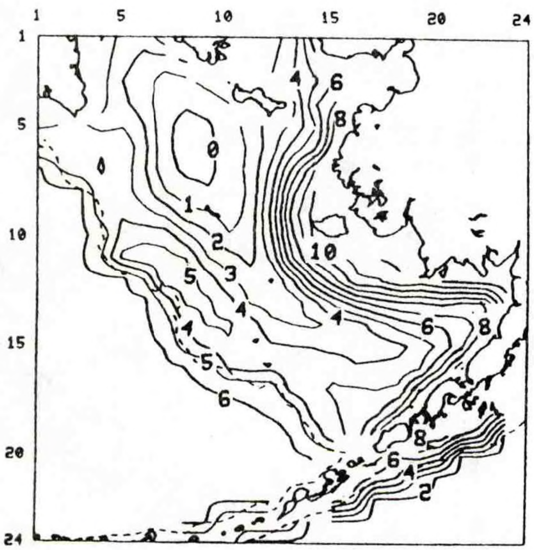

SEPTEMBER

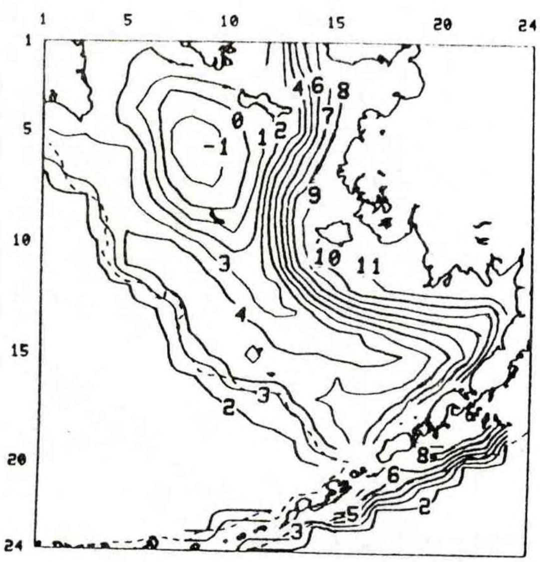

OCTOBER

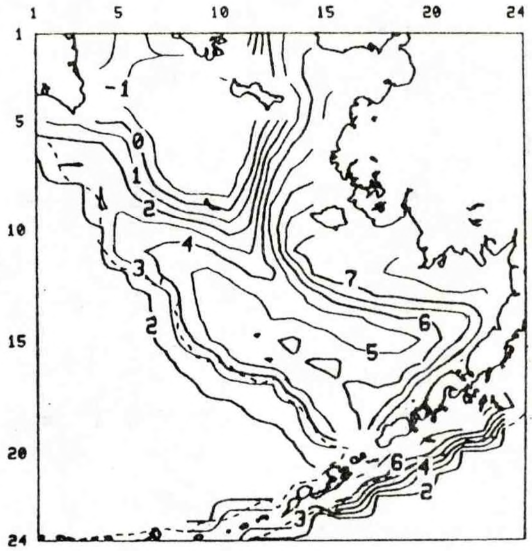

NOVEMBER

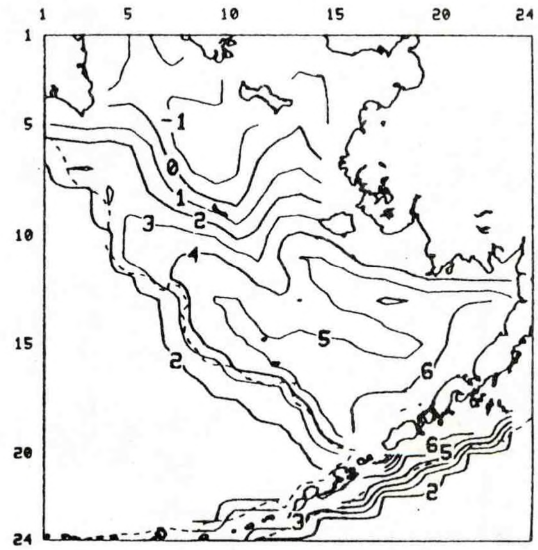

DECEMBER

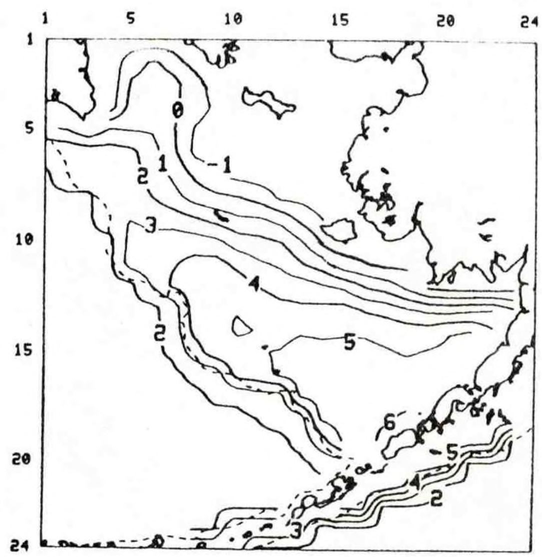

JULY

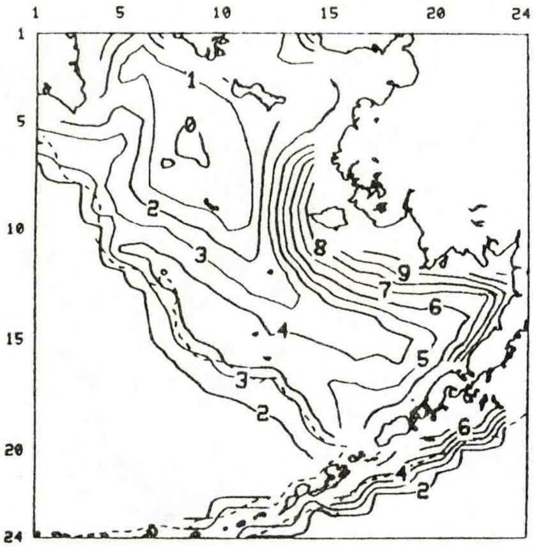

AUGUST

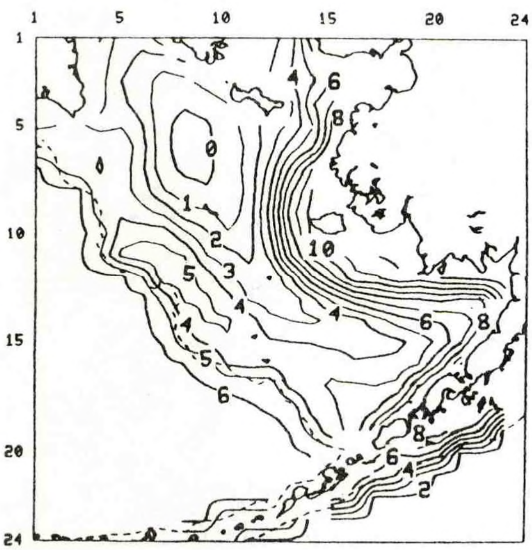

SEPTEMBER

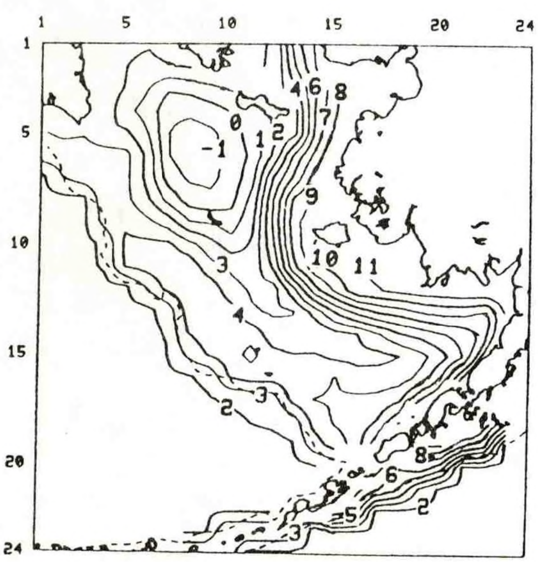

OCTOBER

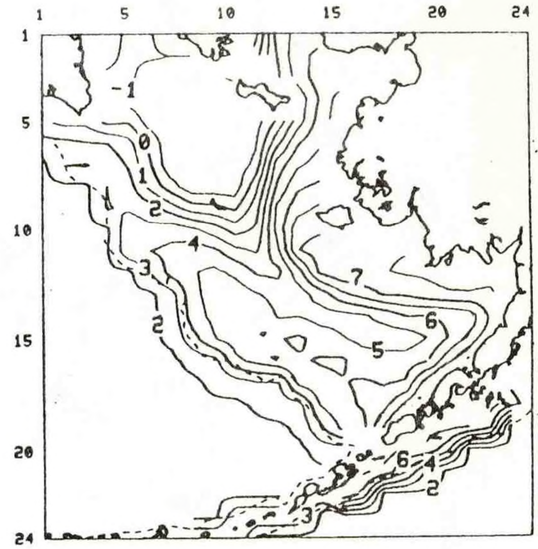

NOVEMBER

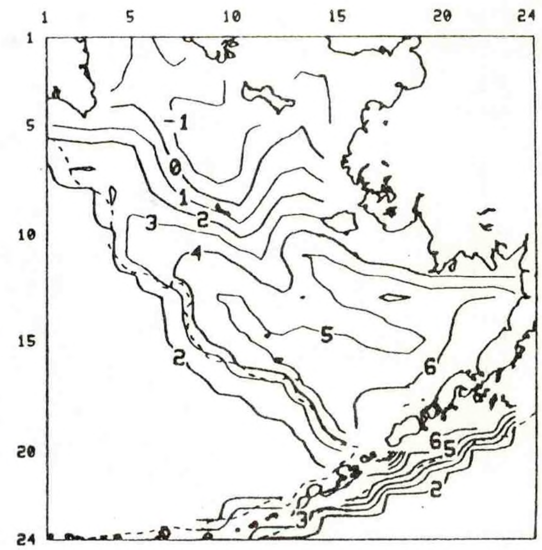

DECEMBER